Temperature Dependent Sulfate Transport in Aquatic Sediments

A Thesis
SUBMITTED TO THE FACULTY OF
UNIVERSITY OF MINNESOTA
BY

Will D. DeRocher

IN PARTIAL FULFILLMENT OF THE REQUIREMENTS
FOR THE DEGREE OF
MASTER OF SCIENCE

Nathan W. Johnson Ph.D.

November 2014

Acknowledgements

The following people have been key participants in the preparation and execution of this experiment and report: Dr. Nathan Johnson, (University of Minnesota Duluth) and, Dr. Edward Swain and Phil Monson, (Minnesota Pollution Control Agency), were instrumental throughout the entire process, providing key insight into the experimental design, presentation of results, and helping hands through the countless, and sometimes cold, hours of sampling, data processing, and editing. I would also like to thank Ryan Armstrong, an undergraduate student at the University of Minnesota Duluth, Brian Beck, and Sean Rogers of LacCore UMN, for providing much appreciated assistance throughout the sample collection and processing which aided in the smooth progression of this experiment.

ABSTRACT: Sulfate, released to overlying waters from natural sources and human activity, has the potential to be reduced to sulfide within the anoxic environments of aquatic sediments and negatively impact the growth of aquatic vegetation. Wild Rice is of particular concern within Minnesota as it is both an economic and cultural resource within the state. This study was conducted to characterize the temperature dependence of sulfate transport, via diffusion, between overlying waters and sediment porewaters through the use of laboratory experimentation and mathematical analysis to study the transient response to changes in the overlying water concentration.

Two riverine sediments with contrasting organic carbon content from the St. Louis River watershed in northern Minnesota were characterized for their bulk geochemistry and incubated under laboratory conditions to observe the temperature dependence of ion transport between overlying water and sediment porewaters. Two identical sets of laboratory microcosms, incubated under warm and cold conditions, were subjected to a sulfate loading phase in which the overlying water was spiked with sodium sulfate to induce a concentration gradient between the sediment porewaters and overlying water. At the end of the sulfate loading phase, the sulfate gradient was reversed by replacing the overlying water with fresh water, causing sulfate to diffuse out of the sediment, back into the overlying water. During the sulfate recovery phase, sodium bromide was spiked into the overlying water. Bromide, acting as an inert chemical tracer, provided a diffusion-only baseline with which to compare to reactive sulfate. The anion concentrations in the overlying waters were closely monitored to quantify changes in the concentration through the sulfate loading and recovery phases. Non-destructive porewater samples were collected using Rhizon® soil moisture samplers to measure concentrations of sulfate, bromide, ferrous iron, pH, and sulfide at discrete depths in the sediment during key times after changes in surface boundary conditions.

Averaged results from both the high and low organic sediments showed sulfate transport occurred 49% faster out of the overlying waters into the sediments at 23°C when compared to 4.5°C. Estimated rates of sulfate reduction at 4.5°C were on average, 40% of those estimated at 23° C. After seven weeks of recovery from the sulfate loading, porewater sulfate concentrations in the warm microcosms had dropped back to ambient levels while slightly elevated sulfate levels were still noticed within the cold microcosm porewater. Even though more sulfate diffused into the warm sediments, the cold sediments retained the sulfate for a significantly longer period of time after the change in boundary layer conditions due to the retarded rates of diffusion and reaction. The longer the sediment is exposed to elevated sulfate levels a greater potential exists for the wild rice seed within the sediment to be exposed to sulfide.

Table of Contents

Table of contents

Acknowledgements i
List of Tables iv
List of Figures v
Introduction 1
Materials and Methods 6
Experimental methods and experimental setup 6
Experimental setup 8
Experimental treatments 9
Field and laboratory sampling methods 10
Analytical methods 11
Results 11
Equilibration phase 12
Phase I – Sulfate Loading Phase 13
Phase II – Sulfate recovery Phase/ Bromide loading Phase 18
Relevance of lab measurements to field conditions 21
Mass transport comparison of sulfate and bromide 22
Observed sulfate loss in overlying waters 22
Conclusions and implications 27
Future Studies 30
References 32
Appendix A. 36
Appendix B 48
Appendix C. 48

List of Tables

Table 1 Characteristics of sediment retrieval sites 7
Table 2 Sulfate and bromide manipulations in overlying water. 9
Table 3 Equilibration Phase averaged anion concentrations for overlying water. 13
Table 4 Bromide mass balance 25
Table 5 Sulfate mass balance 26
Table 6 Sulfate reduction 27
Table 7 Monod sulfate reaction parameters 27
Table 8 Outline of experimental schedule 36
Table 9 Overlying water sulfate concentrations, Partridge River 37
Table 10 Overlying water sulfate concentrations, North Bay 38
Table 11 PR Cold porewater Sulfate concentrations 40
Table 12 PR Warm porewater Sulfate concentrations 40
Table 13 North Bay Cold porewater sulfate concentrations 42
Table 14 North Bay Warm porewater sulfate concentrations 42
Table 15 Sulfate Reaction terms obtained from Pallude and Cappellen, 2005 48

List of Figures

Figure 1 Sediment Retrieval Sites 7
Figure 2 Sediment homogenizing process 7
Figure 3 Experimental microcosm components 9
Figure 4 Equilibribration Phase porewater sulfate concentrations 13
Figure 5 23°C North Bay and 23°C Partridge river microcosms 14
Figure 6 Phase I overlying water and porewater chemistry 16
Figure 7 Porewater sulfate concentrations in microcosms during Phase I and Phase II 17
Figure 8 Overlying water anion concentrations of sulfate and bromide 20
Figure 9 Overlying water and porewater chemistry in warm and cold microcosms 20
Figure 10 Visual example of summation of decrease in overlying water concentration. 23
Figure 11 Example of integrating the area under the concentration-depth curve 24
Figure 12 Porewater sulfate concentrations during equilibrium phase 39
Figure 13 Porosity measurements 43
Figure 14 pH measurements 43
Figure 15 Partridge River porewater iron measurements 44
Figure 16 Partridge River porewater sulfide measurements. 44
Figure 17 North Bay sediment porosity measurements 45
Figure 18 North Bay sediment pH measurements 45
Figure 19 North Bay porewater iron measurements 46
Figure 20 North Bay porewater sulfide measurements 46
Figure 21 Partridge River AVS results 47
Figure 22 North Bay AVS results 47

List of Equations

Equation 1: Organic Carbon and sulfate Reaction ……. …… 2
Equation 2: Q_{10} Reaction Adjustment for Temperature Dependent Reactions……... 4
Equation 3: Temperature adjustment for Ionic Diffusion Coefficients ……..... 4
Equation 4: Summation of Mass Loss in the Overlying Water ……..... 23
Equation 5: Summation of Mass Accumulation in the Porewater ……... 24
Equation 6: Monod Sulfate Reduction Model …… 26

Introduction

Sulfate is a naturally occurring form of oxidized sulfur that is released into the environment from both natural and anthropogenic sources; it readily dissolves into water, making it mobile in lakes, streams, and other aquatic systems (MPCA, 1999). Major sources of sulfate loading to surface waters include waste water treatment effluent, industrial excavation sites, industrial discharge, atmospheric deposition from acid rain, and decomposition of organic matter (Spears, 2005).

Elevating sulfate levels in the overlying water of natural systems which presently have low sulfate exposure, has the potential to be damaging to ecosystems, as elevated sulfate has been linked to elevated mercury methylation, increased phosphorus mobilization, and higher levels of sulfide (Scheidt and Kalla, 2007). As a natural and cultural resource within Minnesota, wild rice *(Zizania aquatica or Zizania palustrus)* are protected by the state for commercial and societal purposes (MPCA, 2013). With this goal, Minnesota's Pollution Control Agency has established water quality standards to regulate the release of sulfate that may adversely affect wild rice production in Minnesota waters. This study was conducted as a part of a larger effort by the Minnesota Pollution Control Agency (MPCA) to better understand the relationship between sulfate levels in surfaces waters and its effects on wild rice.

Minnesota's 10 mg/L sulfate standard (about 0.10 mM) for class 4A designated waters "used for the production of wild rice during periods when the rice may susceptible to damage by high sulfate levels," (Minn. R. 7050.0224, subpt. 2) is based on the 1930-1940's work of Dr. John Moyle who determined that "No large stands of rice occur in water having sulfate content greater than 10 ppm (parts per million), and rice generally is absent from water with more than 50 ppm" (Moyle, 1944). With funding from the Legacy Amendment Bill, provided by the Minnesota Legislature in 2011, the MPCA has organized several studies to explore the relationship between sulfate and inhibited wild rice growth. The working hypothesis is that chemically reduced sulfate, or sulfide, is the chemical species that is detrimental to the growth of wild rice. Sulfides have been identified as toxic to several other types of rice and aquatic vegetation (Armstrong and Armstrong, 2005, Gao et al., 2003, Smolders et al., 2003).

Under anoxic conditions, sulfate acts as a terminal electron acceptor for bacterial respiration of organic matter (Orem et al. 2011). Key to this reaction is the availability of sulfate and a nutrient source (organic carbon) to the bacteria and the byproducts of this reaction are

energy, sulfide, and bicarbonate (Eqn. 1; Pallud and Van Capellan, 2006). Previous studies have found negative correlations between sulfate loading and aquatic vegetation production due to sulfide toxicity (Allam & Hollis, 1972; Koch & Mendelssohn, 1990). In a study conducted in the Florida everglades (14-65 mg L^{-1} dissolved organic matter), elevated sulfate levels in the overlying water (approx. 0.6 mM) have been linked to sulfide toxicity of native species such as sawgrass and the invasion of non-native cattails (Orem, 2007). In another Everglades study, 0.21 mM sulfate in the overlying water correlated to 0.03 mM sulfide in the porewater (Gilmour et. al, 2007).

$$2CH_2O + {SO_4}^{2-} \leftrightarrow HS^- + H^+ + 2{HCO_3}^- \qquad \text{(Eqn. 1)}$$

Sulfate, a dissolved ion, can be transported into sediment porewaters through either advective ground water movement, or diffusive flux. As advective fluid flows are highly spatially variable, they have not been considered within the scope this study. Diffusive fluxes however, occur only as a result of a concentration gradient and can occur wherever such a gradient exists. Several studies have previously been conducted to quantify diffusional sulfate fluxes both under laboratory and field conditions. Sulfate flux measurements between of 12-118 μmol m^{-2} day^{-1} were made during an *in situ* study in Little Rock Lake, WI (24-32% organic carbon measured in the sediment), by increasing the sulfate concentration in the overlying water to 70 μM with concentrated sulfuric acid (Urban et al., 2001). In a study conducted with sediments collected from the Danish coast and incubated under 4° C laboratory conditions, 20% differences in sulfate diffusion rates were observed based on the sediment porosity. Fluxes of 23 μmol m^{-2} day^{-1} were measured in sediments with 75% porosity and fluxes of 34 μmol m^{-2} day^{-1} in sediments with 90% porosity (Iversen & Jorgensen, 1992).

Once the sulfate has moved into the porewaters, bacteria utilize it within their respirational processes, converting it to sulfide (Eqn. 1), and it is sulfide that is presumed to have damaging effects on wild rice production. Area-normalized sulfate reduction rates for oligotrophic lakes have been observed between 3-21 mM m^{-2} day^{-1} (1.4-4.0% carbon content within the sediment; Bak & Pfenning, 1991) and 0.6-7.4 mM m^{-2} day^{-1} for eutrophic lakes (Sinke et al., 1992; Steenbergen et al., 1993). These bulk rates, which depend on sulfate supply and reaction, indicate how quickly sulfate can be reduced to sulfide within the anoxic regions of freshwater aquatic sediments.

Sulfate concentrations in the overlying water, however, do not directly correlate to sulfide concentrations in the porewater. Sediments have differing levels of buffering capacity against the buildup of porewater sulfide (Heijs et al., 1999). Sulfate transport from the overlying water and sediment permeability can affect sulfate supply to the sediments. Temperature, oxygen levels, iron, nitrate, and organic content all play a role in biological sulfate reduction rates. (Koschorreck & Wendt-Potthoff, 2012; Holmer & Storkholm, 2001). When sulfate penetrates into sediment, and is converted to sulfide, dissolved metals, such as ferrous iron, can bind it in pH-dependent FeS and FeS_2 precipitates (Berner, 1970; de Wit et al., 2001; Rozan et al., 2002; Heijs and van Gemeren, 2000; Raiswell & Canfield, 1998; Van der Welle et al., 2007). Sulfide oxidation also stimulates the reduction of ferric iron to ferrous iron under anoxic conditions, providing additional dissolved sulfide buffering capacity within the sediment (Giordani et al., 1996; Stal et al., 1996).

pH of the reducing environment also impacts the nature of dissolved sulfides. Within natural systems, the respiration of sulfate can either produce hydrogen sulfide (H_2S) or sulfide (HS^-) depending on the pH (Below pH 7, H_2S is the dominant species). Although it is not presently known which form is toxic to wild rice, H_2S is a known inhibitor of enzymes used for aerobic respiration, iron containing enzymes, and the uptake of nutrients (Allam & Hollis, 1972), all of which are important to the growth and reproduction of plants, including rice. Sediment porewater pH of 5 presents the lower operational bound of sulfate reducing bacteria. Conditions are conducive to the presence and production of H_2S between pH 5 and 7, which is the typical within natural systems, (Kösel et al., 2001).

Temperature has a direct effect on biological processes, including sulfate reduction, which can be separated from the effect of temperature on diffusion in conditions where sulfate reduction is not limited by sulfate supply. Temperature not only changes the metabolism rate of the bacteria, but it also slows the bacterial growth rates and the transport of sulfate from the overlying water, potentially limiting the bacterial respiration (Holmer & Storkholm, 2001). A direct correlation between temperature and growth rate was observed by White et al., in their 1990 study investigating the effects of temperature on biological growth and production rates. As temperature increases, the biological growth rate followed (Eqn. 2; Baig & Hopton, 1969). Although biological production rates are primarily based on the abundance of bacteria, temperature impacts the production rate as well (White et al., 1990). A common method to adjust biological reaction rates for a $10^{\circ}C$ temperature change (Q_{10}, Eqn. 2) was used to compare

expected and reported reduction rates for freshwater sediments at 4.5°C and 23°C (Baig & Hopton, 1969).

Temperature not only affects the biological activity within the sediment, but also the chemical activity as well, since ionic diffusion is based on the random movement of charged molecules (energy state), a decrease in temperature decreases the energy within the system, thereby decreasing the overall diffusive transport within that system.

The Nernst expression (Eqn. 3) for the self-diffusion coefficient, which is the same as diffusion in an infinite dilution, is directly related to the absolute temperature of the system (Robinson and Stokes, 1959; Yuan-Hui and Gregory, 1973). Theoretically, sulfate diffusion at 4.5°C (occurring at 5.9 E-06 cm^2 sec^{-1} in free solution) is nearly half of what occurs at and 23.0°C (occurring at 1.02 E-05 cm^2 sec^{-1} in free solution; Boudreau, 2003). In-situ observations of sulfate reduction rates made in the Northern Adriatic Sea, in which temperature affects SO_4 diffusion and reaction, indicated a nearly fourfold increase in sulfate reduction during the summer (14.9 mM m^{-2} d^{-1}) when compared to the winter (3.9 mM m^{-2} d^{-1};Azzoni et al., 2005).

$$Q_{10} = \left(\frac{R_2}{R_1}\right)^{\left(\frac{(T_2 - T_1)}{10}\right)} \quad \text{Eqn. 2}$$

Where:
Ri = Temperature dependent reaction term
T_i = Respective temperature

$$D_j^0 = \frac{RT\lambda_j}{abs(z_j)F^2} \quad \text{Eqn. 3}$$

Where:
D_j^0 = Self-diffusion coefficient
λ_j = Equivalent conductive of ion_j
$abs(z_j)$ = Absolute value of the charge on ion_j
R = Gas constant
T = Absolute temperature
F = Faraday constant

This laboratory experiment investigated the diffusion of sulfate (SO_4^{-2}) and bromide (Br^-) into the top 10 cm of two contrasting freshwater riverine sediments under warm (23°C) and cold (4.5°C) temperatures. When diffusion from the overlying water is the major transport mechanism of sulfate, its penetration is not common beyond 10 cm in freshwater sediments, as discussed

below. Active bacterial sulfate reducing colonies, driven by sufficient organic carbon, typically consume nearly all dissolved sulfate mass between 0 and 10 cm below the sediment water interface (Molongoski & Klug, 1980; Smith & Klug, 1981; Cook & Schindler, 1983; Ingvorsen et al., 1981; Sass et al., 1997). As such, sulfate transport and geochemical analyses for this experiment were limited to the top 10 cm of the incubated sediments, even though the sediment depth was >30 cm to eliminate any effects from the bottom of the experimental microcosms. For the experimental portion of this study, two characteristically different sediments - high organic and low organic - were retrieved from the St. Louis River watershed and incubated for seven months at two temperatures. Throughout the study, temperature remained constant and the upper boundary sulfate concentrations was changed to mimic natural systems that see seasonal variation in sulfate concentrations due in part to permitted winter releases of sulfate laden water. The overlying water and sediment porewater were monitored throughout the experiment to record the sulfate mass loss from the overlying water and accumulation in the sediment porewater. Since rates of sulfate reduction were not directly quantified in this study, they were inferred from observations of mass loss from the overlying water and accumulation in the sediment porewater. Water overlaying the sediment in each microcosm was continuously mixed and aerated to eliminate chemical gradients above the sediment-water interface in an effort to mimic conditions in a shallow natural stream that might receive sulfate-enriched discharges.

One of the objectives of this study was to observe the extent to which biological reduction and molecular diffusion depend on temperature. The temperature settings selected for this experiment were chosen based on summer and winter water temperatures in the St. Louis River. Presently the MPCA permits selected industrial sites that generate large amounts of sulfate rich water to discharge this water to particular streams during the winter months. Sulfate released during the winter theoretically has less potential to be converted to sulfide within the sediment due to slower rates of diffusional transport and bacterial reduction. Even though the sulfate transport into the sediment is slowed during colder winter temperatures, the transport out of the sediment, once permitted discharges cease, is also slowed. This has raised concerns about the impact of winter sulfate releases as the sulfate remaining in the porewater may be available to bacteria, and subsequently reduced to sulfide, as the sediment warms to ambient spring temperatures. A sulfate recovery phase was incorporated into this experiment, designed to simulate a reversal of the sulfate gradient as it would occur in the time following a halt in sulfate-elevated discharges at the end of winter. The goal of this phase was to observe the time-

dependent response of sulfate in the sediment porewaters to determine the how long sediment in a river system may be exposed to residual sulfate after the winter loading cutoff.

Materials and Methods

Experimental methods and experimental setup

In January 2013, approximately 50 L of sediment was recovered from the top 10 cm of each of two river beds within the sulfate-impacted St. Louis River watershed (Figure 1) by scooping the sediment from the river bed using fine mesh screens. The Partridge River sampling location was a backwater location in a tributary near the headwaters of the St. Louis River on the East-central portion of the Mesabi Iron Range in Northern Minnesota. The Partridge River site provided sediment from a slow-moving part of a sulfate-impacted river (Berndt & Bavin, 2009) where wild rice had been observed in recent years. The second sampling location, North Bay, was near the mouth of the St. Louis River, approximately 15 km upstream from the entrance into Lake Superior in the St. Louis River Estuary. The North Bay site, a protected bay away from the main channel, provided lower organic sediment from a location where rice has also been observed in recent years (Table 1, Figure 1).

Each sediment sample was homogenized by compositing the sample in a 135 L drum, removing sticks, rocks, clams and other debris, and gently folding it over with an electric paddle mixer for 10 minutes at 15-20 rpm. Once thoroughly mixed, the sediment was proportioned into microcosms to a depth of 30 cm and consolidated using a concrete vibration table to minimize the presents of air pockets (Figure 2). Sediment porosity within the laboratory microcosms was measured half way through the experimental loading phase within two sacrificial microcosms and at the end of the experiment by coring the laboratory microcosms (Appendix A, Figures 13 and 17). The overall homogenization process took approximately 90 minutes for each of the sediments. Water retrieved from the respective sites was pumped into microcosms and capped the sediment with a 10 cm layer of water. The microcosms were then transported to their respective temperature controlled environments and allowed to adjust to laboratory conditions for nine weeks prior to beginning the experimental phases (Table 2).

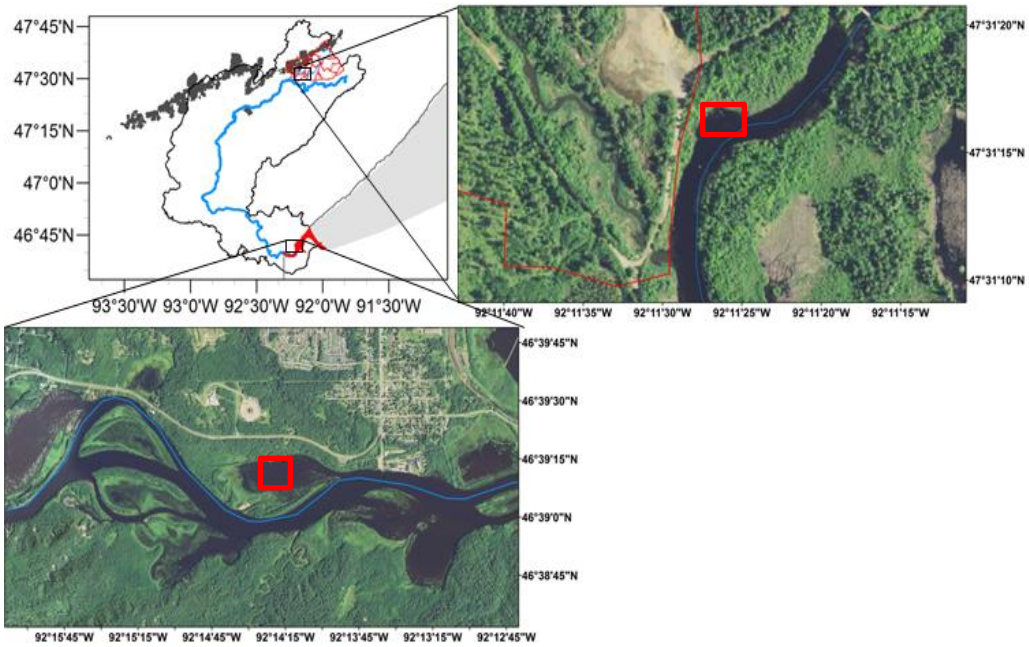

Figure 1 Sediment Retrieval Sites. Upper: The northern site, Partridge River and Lower: the southern site, North Bay.

Figure 2 Sediment homogenizing process, Left: mixing drum, Middle: sediment proportioning, and Right: sediment consolidation.

Table 1 Characteristics of sites where experimental sediments were retrieved.

	Latitude	Longitude	Overlying SO_4^{-2*} mM	In situ Porosity^{+}	Carbon Content
Partridge River	47° 31. 271'	-92° 11. 410'	0. 46	91%	5.65% (+/- 1.7)^
North Bay	46° 39. 188'	-92° 14. 225'	0. 16	74%	3.03% (+/- 0.13)^

***Site avg. at time of sediment collection calculated according to porosity eqn. in appendix B**
$^{+}$0-10 cm sediment average
^n=9, carbon content quantified on homogenized sediment at close of experiment

Experimental setup

Microcosms consisted of polycarbonate plastic tubing (60 cm height, 20 cm ID, 0.3 cm wall thickness) with a sealed bottom and Rhizon® soil moisture samplers fixed and sealed at approximately 2 cm depth intervals along microcosm's side to minimize the influence of one filter on another (Figure 3, Seeberg-Elverfeldt et al., 2005). The Rhizon® samplers were used to take 3 mL samples of porewater at specific times throughout the experiment for the monitoring of sulfate, bromide, pH and ferrous iron concentrations within the sediment (Figures 14-19, Appendix A).

Microcosms were loosely capped with an acrylic plate to avoid evaporative losses. An aeration system was also included to maintain well mixed conditions analogous to a natural river system by avoiding the development of anoxic conditions in the overlying water. An aquarium pump was used to push air for the aeration system through an activated carbon filter to remove airborne contaminants, then through a HEPA filter to remove particulate matter, and finally through a sealed flask of deionized water to hydrate the air (Figure 3). The microcosms were incubated under dark, temperature-controlled conditions throughout the experiment to minimize disturbances and to eliminate variables such as photosynthesis. Three microcosms filled with Partridge River Sediment were incubated at 4.5° C and three identical microcosms were incubated at 23°C for the duration of the experiment. An analogous set of microcosms were constructed and incubated using homogenized sediment from North Bay and incubated at the same temperatures.

Throughout the experiment; the overlying water was exchanged for fresh site-specific water that had been amended with either sulfate or bromide. Fresh water was slowly pumped over the sediment when refilling to minimize sediment agitation. Due to an unforeseen rise in sulfate concentration within the warm Partridge River microcosm, which was presumed to be caused by the oxidation of sulfides within the sediment, the overlying water in these microcosms was exchanged more frequently than North Bay (Appendix A, Table 8; Figures 6, 8).

Figure 3 Experimental microcosm components. Top: Air pump, activated carbon filter, HEPA filter, sealed flask of deionized water and manifold delivering air to overlying water in microcosms. Lower Left: Test microcosm filled with water prior to addition of sediment. Lower Right: rhizon: tubes extending from sediment filled microcosms.

Experimental treatments

The experimental portion of the study occurred in two phases to quantify the transport of sulfate and bromide across the sediment-water interface resulting from diffusional transport (Table 2). Phase I was initiated after a nine-week equilibration period for the sediment-filled microcosms at either 4.5 °C or 23 °C. During the equilibration phase, sulfate concentrations in the overlying water were monitored weekly, and the overlying water was replaced with site water when necessary to maintain low sulfate concentrations.

Table 2 Sulfate and bromide manipulations in overlying water during experimental phases.

Experimental Phase	Overlying water Sulfate Amendment	Overlying water Tracer Amendment	Length
Equilibration	None	None	9 weeks
Phase I	3.0 mM	None	11 weeks
Phase II	None	Bromide (0.25 mM)	8 Weeks

Phase I, the sulfate loading phase, was initiated by replacing the overlying water with fresh site water amended with sodium sulfate (3.0 mM sulfate; Table 2). Sulfate was amended at the outset of Phase I and re-spiked three times throughout the 11 week loading phase. The sulfate

amendments occurred relatively infrequently to enable the quantification of sulfate mass lost from the overlying water of each individual microcosm through weekly overlying water measurements. The amended sulfate concentration was 3.0 mM since several streams contributing to the main stem of the St. Louis River regularly contain such sulfate concentrations during particular times of the year (Berndt & Bavin, 2012). Sulfate spikes to overlying water induced a sharp gradient between the surface and porewaters, providing a driving force for diffusional mass transport into the sediment porewater from the overlying water. The decrease in overlying water sulfate concentrations during Phase I provided a means to estimate the cumulative sulfate mass that had been transported into the sediment over the course of the experiment.

During the nine weeks of Phase II, the sulfate recovery phase, the overlying water was amended with sodium bromide and the sulfate was maintained at low concentrations to reverse the sulfate gradient between the overlying water and porewaters. The overlying water was exchanged weekly for the first three weeks of Phase II to maintain the low sulfate conditions as the bulk of the sulfate migrated into the overlying waters, and then less frequently as the sulfate transport out of the sediment slowed (Appendix A, Table 8). During this phase, the direction of sulfate transport reversed (out of the sediment), though biological sulfate reduction continued to consume sulfate in the sediment porewaters

Field and laboratory sampling methods

While retrieving the bulk sediment to construct microcosms, 7-cm diameter polycarbonate cores were collected, transported to the lab, sectioned into 1-2 cm depth intervals and, homogenized in an anoxic chamber for a high resolution analysis of *in situ* porosity, acid volatile sulfide (AVS), ferrous iron, and dissolved sulfide. Porewater samples were taken by compositing sediment from replicate intact cores collected at each site at similar depth s extracting the porewater using Rhizon filters (Seeberg-Elverfeldt et al., 2005). Two additional laboratory microcosms were constructed at the beginning of the experiment and maintained until the end of Phase I, at which time similar high resolution sampling for sediment chemistry was conducted. At the end of the experiment, the same high-resolution sampling was conducted on all laboratory microcosms to ensure experimental consistency and provide a comparison between laboratory and in situ conditions (Appendix A, Figures 13-22).

Basic measurements of the overlying water including, water depth, temperature, conductivity, pH, and dissolved oxygen, were made twice a week using a measuring tape and

calibrated Hydro-Lab Sonde to ensure consistent oxygenated conditions throughout the test. Samples of the overlying water (10 mL) were collected, filtered through a 0.45 µm polyethersulfone (PES) filter, and analyzed weekly using ion chromatography in order to monitor the transport of sulfate both into and out of the sediment. Porewater samples (<3 mL) were taken from each rhizon at the beginning and end of each experimental phase to conduct a stratigraphic porewater analysis of the pH, ferrous iron, and sulfide concentration along the depth profile of the sediment. The sample volume was dictated by the radius of influence created by the rhizon filters (~0.5 cm; Seeberg-Elverfeldt et al., 2005). Porewater samples taken at intermediate times in experimental phases were only to quantify sulfate and tracer ion concentrations (Appendix A, Table 11-14).

Analytical methods

Anion concentrations for the overlying waters and porewaters were quantified following filtration (0.45 µm PES filter, and 0.2 µm Rhizon® filter respectively) using ion chromatography, method 4110 C (Eaton et al.3500 Fe-B, 2005) with chemical suppression of eluent conductivity on a Dionex ion chromatograph using the Chromelion software for peak integration. Dissolved ferrous iron (Fe^{2+}) was quantified in filtered porewater samples using the phenanthroline method (Eaton et al. 2005). Reagents were preloaded into vials to immediately preserve the sample and prepare it for analysis using spectrophotometry. Porewater sulfide concentrations were analyzed on filtered samples immediately upon extraction (reagents pre-loaded into vials) using the Hach 8131 method, an adaptation of method 4500-S^2-D in Eaton et al. (2005). Detection limits were approximately 0.5 µM for sulfide and 3 µM for iron. For high-resolution solid phase samples from the in situ and laboratory cores, ASTM D2216-10 and ASTM 854-10 were used to determine moisture content and specific gravity of the sediment respectively. Results from both tests were used to calculate sediment porosity as a function of depth in the sediments.

AVS samples were taken from the composited sediment from specific depth intervals and analyzed by the Minnesota Department of health according to ASTM D2216. Samples taken to measure *in situ* dissolved sulfide were also analyzed by the Minnesota Department of Health according to the SM4500-S2J method for dissolved sulfide.

Results

Over the course of the experiment, the overlying water in the 23° C microcosms filled with Partridge River sediment clouded and the sulfate concentration rose quickly after a water exchanges. Both trends persisted through the equilibration, first, and second phases of this study

despite regular water exchanges. The clouding of the water and the unforeseen rise in sulfate concentration within the equilibration phase was likely due to oxidation the sediment underwent in the transition from the field to microcosms. Increases in overlying water sulfate later in the study were most likely due to benthic organisms dwelling in the sediment, churning the upper layers of the sediment, and exposing solid phase sulfide to the oxygenated water, and subsequently releasing it as sulfate (Figure 6). As the sediment collected for this study was comprised of the top ten centimeters of riverine sediments, it is likely that benthic organisms were unintentionally collected with the sediment and became active as the sediment warmed, as has been observed in other studies (Palmer et al., 1997; Covich et al., 2004; Mermillod- Blondin, 2011). Though burrowing was observed in both warm sediments, the Partridge River had a greater potential for sulfide oxidation due to the higher amounts of sulfides contained within the sediment (Figures 21 and 22). The activities of benthic communities within the sediment have the potential to lower the porewater pH, which increases the tendency for iron species dissociation (Caliman et al., 2007; Gerino et al., 2006; Kristensen, 2000; Lewandowski et al., 2007; Mermillod-Blondin & Rosenberg, 2006). Although the results from the 23°C Partridge River microcosms were different from the analogous North Bay microcosms, the transport trends were still analyzed and compared to the North Bay results.

Equilibration phase

Sulfate concentrations were less than 0.5 mM in sediment porewaters during the equilibration phase, except in the top 3-5 cm of the warm Partridge River sediments, where sulfate concentrations were noticeably higher and assumedly being transported to the overlying water. In the cold Partridge River, sulfate was uniformly elevated in porewaters at all depths (Appendix A, Figure 12). A possible explanation for elevated sulfate in cold Partridge River microcosms was that residual sulfate from the oxidation of sulfide minerals during microcosm construction elevated sulfate in Partridge River porewaters, as has been observed by De Jonge et al. (2012). Reduced biological rates of sulfate reduction in the cold incubated microcosms likely allowed the sulfate to persist in sediment porewater longer than in the warm incubated microcosms. The nearly uniform decrease in porewater sulfate from 2.1 to 1.0 mM over a 4 week period prior to the initiation of Phase I in cold Partridge River microcosms (Appendix A, Figure 12) suggests a sulfate reduction rate of approximately 37 μM day^{-1} which is on the low end of the range of maximum rates reported by Pallud and Van Cappellen (2010) for freshwater sediment at 21° C (300 – 950 μM day^{-1}) and temperature adjustments of 2-4 times slower per 10 °C drop in temperature, as suggested by Fossing et al. (2000) and Pallud and Van Cappellen (2006).

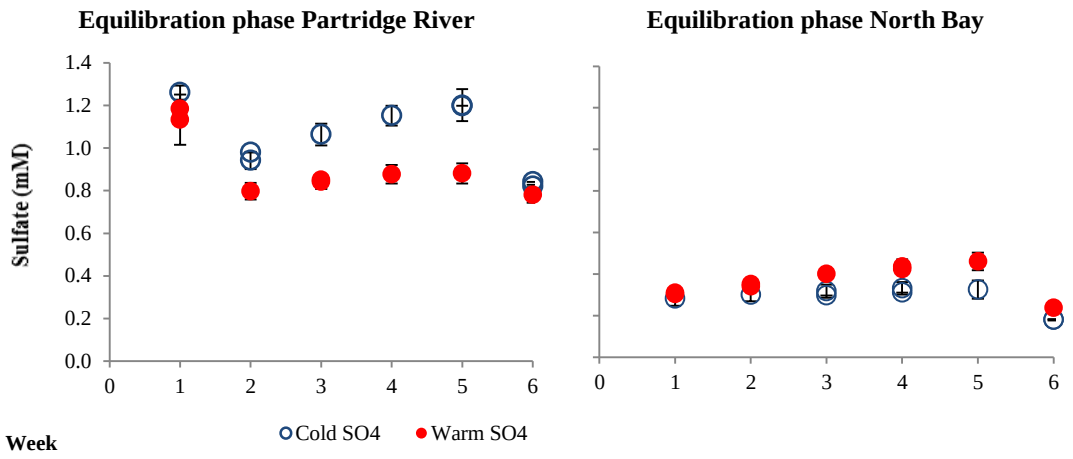

Figure 4 Equilibribration Phase porewater sulfate concentrations in warm and cold microcosms. Left: Partridge River, Right: North Bay. Multiple data points for one week indicate additional sampling during the week due to overlying water replacements. Filled symbols represent measurements made in 23°C Microcosms, hollow symbols represent measurements made in 4.5°C microcosms.

Table 3 Equilibration Phase averaged sulfate concentrations for overlying water.

	4. 5°C	**23°C**
Partridge River sulfate (mM)	1.05	0.88
North Bay sulfate (mM)	0.28	0.35

Phase I – Sulfate Loading Phase

Phase I was an eleven-week period during which elevated sulfate concentrations in the overlying water (Figure 6) were used to characterize rates of sulfate diffusive transport and reaction. Sulfate concentrations began to progressively rise in the 23 °C Partridge River microcosms overlying water about halfway through Phase I (Figure 6, weeks 4-11). This same increase occurred in all three replicates of the warm Partridge River sediments, suggesting it was not an anomalous occurrence. The overlying water was exchanged more frequently to reduce sulfate levels to the 3.1 mM target, but despite the exchanges, sulfate concentrations in excess of 6.5 mM were observed in the 23 °C Partridge River microcosms near the end of Phase I, while the highest concentration in the other microcosms ranged from 3.64-3.80 mM. The overlying water in the 23 °C North Bay microcosms remained fairly clear throughout the experiment, but the water overlying the 23 °C Partridge River sediments became clouded within a matter of days after a water exchange (Figure 5). Borrowing worms were observed tunneling within the

sediment near the sediment water interface and the clouding and rise in overlying water sulfate concentration was attributed to the bioturbation within the sediment.

Due to the rise in overlying water sulfate concentration, observed porewater concentrations were normalized to the average overlying water concentration measured over the week preceding the porewater measurements. By normalizing the porewater concentrations to overlying water concentrations observed at each temperature (which differed markedly between the cold and warm Partridge River microcosms), comparison of temperature-influenced diffusional trends could be made more easily. Normalization had little effect on the North Bay results as the overlying water sulfate concentration remained similar in the cold and warm conditions.

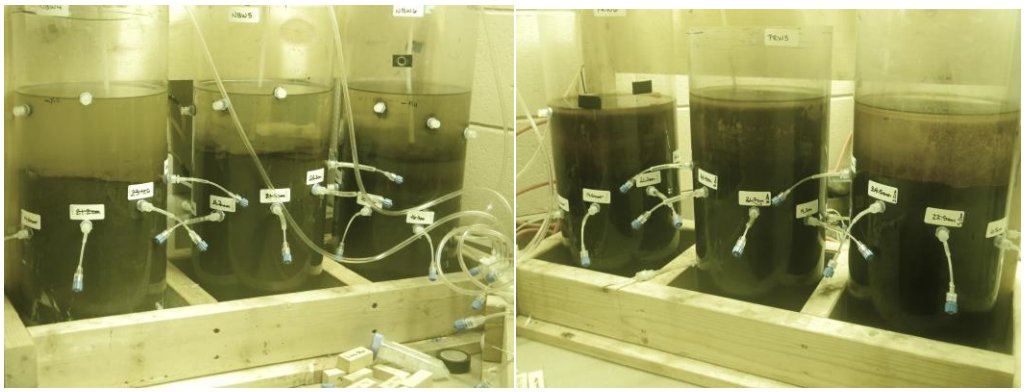

Figure 5 23°C microcosm setup. Left: Triplicate microcosms filled with North Bay sediment. Right: Triplicate microcosms filled with Partridge River sediment, please note the clouding of the water.

Porewater sulfate concentrations were generally less than 0.5 mM at the outset of Phase I in all microcosms (Appendix A, Tables 11-14). The only exception to this was the cold Partridge River porewater, which had approximately 1.05 mM sulfate in porewater as a residual from the equilibration phase. Spiked levels of sulfate were well above the initial concentrations seen in the porewaters (Figure 6 and Appendix A, Figure 12), which effectively established a sharp diffusive gradient between the overlying water and porewater (Figure 7). Sulfate concentrations in the surficial (0-5 cm) microcosm porewaters (normalized to overlying water sulfate concentration from the previous week and three days following when the porewater sample had been taken) increased between 0 and 6 weeks of Phase I; however changes in normalized porewater concentration between the 6th week and 9th week were smaller in both North Bay and Partridge River sediments, indicating that the sulfate gradient between the overlying water and the surficial

porewaters had diminished to the point that diffusion into the sediment matched the reaction within the sediment and near a steady state amount of sulfate in the waters had been achieved. Overlying water sulfate concentrations used for normalization and raw porewater sulfate concentrations are included in the figure legends (Figure 7 Appendix A, Table 9-10).

Over the course of the first nine weeks of the loading phase, an appreciable increase in normalized porewater sulfate concentrations at depths greater than 4 cm were observed within all of the sediments, except the 23°C Partridge river microcosms. Particularly in the North Bay microcosms, it appeared that higher amounts of sulfate were able to penetrate deeper into the sediment in the cold microcosms than in the warm microcosms (Figure 7). Sulfate penetration is a function of diffusion, sulfate gradient, and sulfate reduction. Since a similar sulfate gradient was maintained within both the warm and cold microcosms, and diffusion slows at colder temperatures in a predictable way (Eqn. 3), slower sulfate reduction presents the most likely reason for the observed differences in sulfate penetration depth in the North Bay sediment porewaters.

Sulfate penetration did not exceed 10 cm into the warm sediment, and sulfate concentrations were only marginally above the background levels at 10 cm depth within the cold sediments (<0.21 mM in Partridge River cold and 0.55 mM in North Bay cold sediments, Figure 7 and Tables 11-14 in Appendix A). In contrast, bromide concentrations in excess of 0.1 mM (overlying water concentration ~0.25 mM) were observed in both sets of warm microcosms after 7 weeks of Phase II, the bromide loading phase (Figure 9). Significant (>15%) changes in porewater sulfate concentrations (as compared to the initial conditions) were only observed in the upper 5 cm of sediment for both types of sediment and temperatures. The lack of change in porewater sulfate concentrations at and below 10 cm was expected and is consistent with other freshwater observations (Molongoski & Klug, 1980; Smith & Klug, 1981; Cook & Schindler, 1983). The bromide results indicate that diffusion was not the limiting factor in the sulfate penetration beyond 10 cm, but instead sulfate reaction in both the warm and cold microcosms.

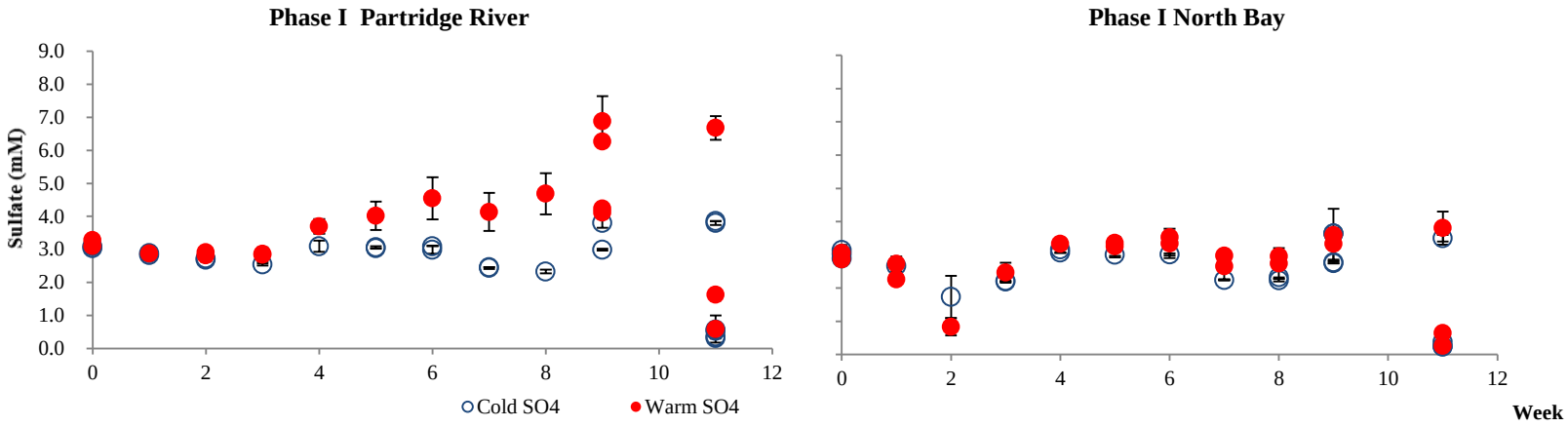

Figure 6 Phase I overlying water sulfate concentrations in the warm and cold microcosms. Left: Partridge River sulfate in the overlying water, Right: North Bay sulfate in overlying water. Multiple data points for one week indicate additional sampling during the week due to sulfate amendments. Filled symbols represent measurements made in 23°C microcosms, hollow symbols represent measurements made in 4.5°C microcosms.

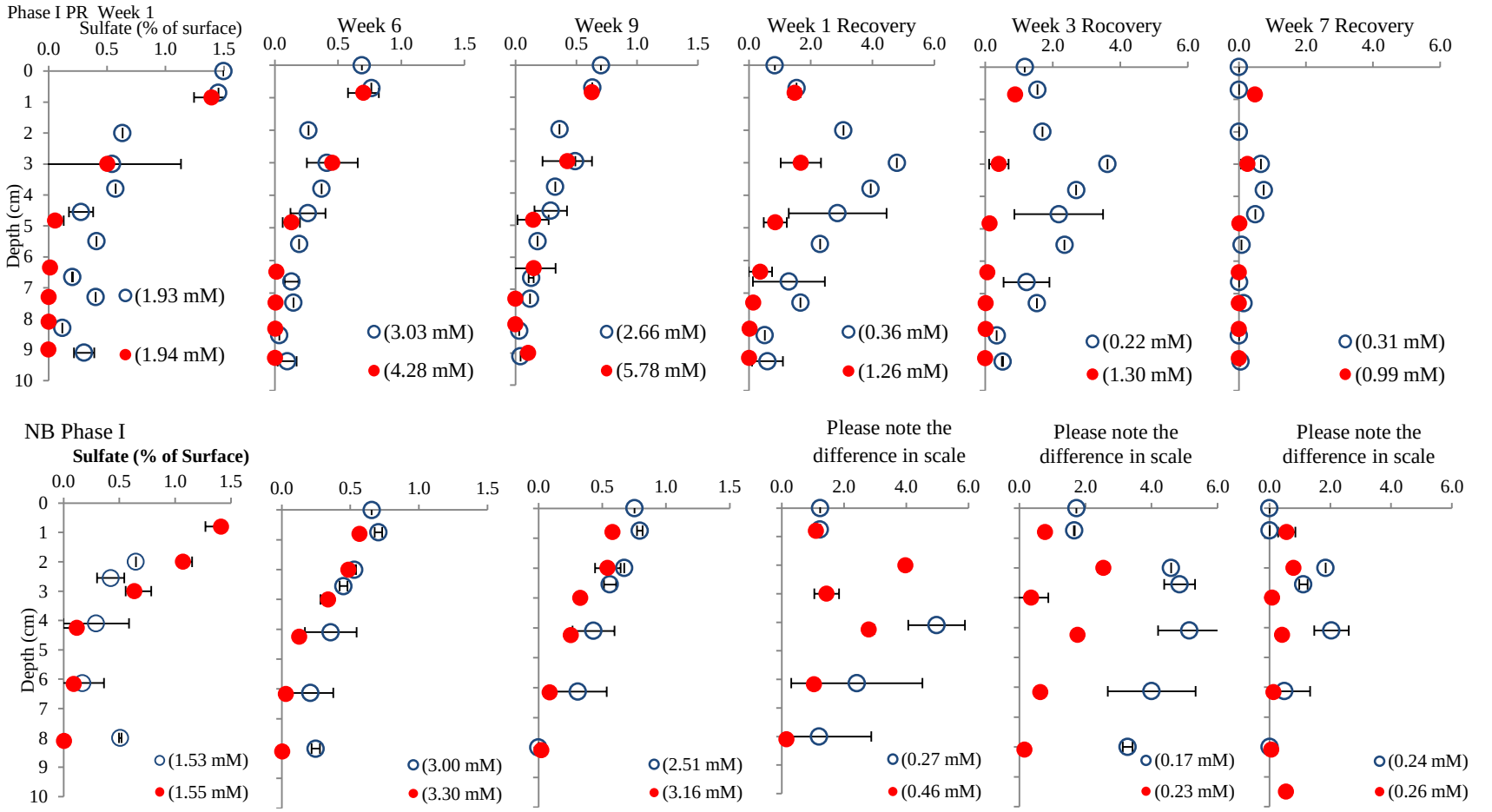

Figure 7 Porewater sulfate concentrations in microcosms during Phase I and Phase II. Top: Partridge River warm and cold porewater sulfate. Bottom: North Bay warm and cold porewater sulfate. Filled symbols represent measurements made in 23°C Microcosms, hollow symbols represent measurements made in 4.5°C microcosms Times denote weeks from the initiation of Phase I (sulfate spike) and scales are porewater concentration as a proportion of overlying water overlying water concentration for the preceding week (mM values in legend). Values denote the average of measurements from replicate microcosms at the specified depth. Horizontal error bars denote the standard deviation of three replicate microcosms.

Phase II – Sulfate recovery Phase/ Bromide loading Phase

At the end of the sulfate-loading phase, overlying water sulfate concentrations were reduced back to ambient levels (approximately 0.11 mM and 0.21 mM for North Bay and Partridge River respectively) by exchanging the sulfate laden overlying waters with fresh site-specific water amended with bromide (Figure 8). The diffusion of bromide was uninhibited by biological reaction and provided an inert chemical tracer to assist in isolating the temperature dependence of diffusion. During the beginning of Phase II, the high concentration of sulfate within the near-surface porewaters diffused back into the overlying waters, and high concentrations of bromide diffused into the sediment.

Within 4 days of beginning Phase II, the concentration of sulfate in the porewaters one centimeter below the sediment water interface sediment dropped to 0.55 mM in the cold Partridge river sediment, less than a third of what was measured in the previous porewater sampling (Figure 7, Week 1 Recovery). A drop from 1.99 mM to 0.17 mM marked an even larger decrease one cm below the sediment water interface in the cold North Bay sediments over the same time period. Decreases in sulfate in the warm sediment porewater for both Partridge River and North Bay were less significant where Partridge River dropped from 1.87 mM to 1.15 mM and North Bay dropped from 1.83 mM to 0.51mM (Figure 7, week 1 of recovery, warm conditions). The porewater sulfate at greater sediment depths took appreciably longer to respond to the boundary change but still decreased due to biological sulfate reduction in the sediments. Even after seven weeks, porewater residual sulfate concentrations could still be observed in both of the cold sediments between 2 and 6 cm. Sulfate concentrations in both of the warm sediments had decreased below 0.21 mM (North Bay) and 0.5 mM (Partridge River; Figure 7). The sulfate concentration in the warm microcosms decreased more quickly due to more rapid diffusion out of the sediment and the accelerated reduction of the sulfate within the sediment at warmer temperatures. The residual sulfate within the cold microcosms is of particular concern in natural systems as the sulfate could be available for bacterial conversion to sulfide in sediment as temperatures rise in the spring, and the biological communities become more active.

Over the course of seven weeks, and uninhibited by reaction, the bromide penetrated beyond 10 cm into the sediment (Figure 9). By the third week, it was evident that the bromide diffusion within the warm Partridge River sediment indeed was more rapid than into the cold sediment. This observation is consistent with the hypothesis that diffusion within the sediment occurs more rapidly as temperature increases, but may also have been accelerated by the activity

of burrowing micro-organisms. By the seventh week, slightly higher bromide concentrations were observed in both the warm North Bay and Partridge River sediments when compared to the bromide concentration in the cold sediments. Though not presented in this thesis, these results are comparable to the predictions made using mathematical models and the diffusion coefficients of bromide in free solution (1.20E-05 cm^2 sec^{-1} at 4.5°C, and 1.88E-05 cm^2 sec^{-1} at 23°C). By fitting a numerical model to the porewater bromide concentrations, free water diffusion coefficients of 8.20E-06 and 1.88E-05 cm^2 sec^{-1} at 4.5°C and 23°C respectively appeared to fit the observations (unpublished results). Effective diffusion coefficients for sulfate are approximately 5.9E -06 and 1.0 E-05 cm^2 sec^{-1} (4.5°C and 23°C respectively; Boudrea, 2003). Even though sulfate diffusion coefficients are slightly lower than bromide, the observed sulfate concentrations would fall well below the concentrations predicted by the diffusion coefficient. Sulfate was not present at 10 cm depth after 9 weeks in any of the microcosms during the loading phase, providing strong evidence that it had been reduced by bacterial activity, even under cold conditions.

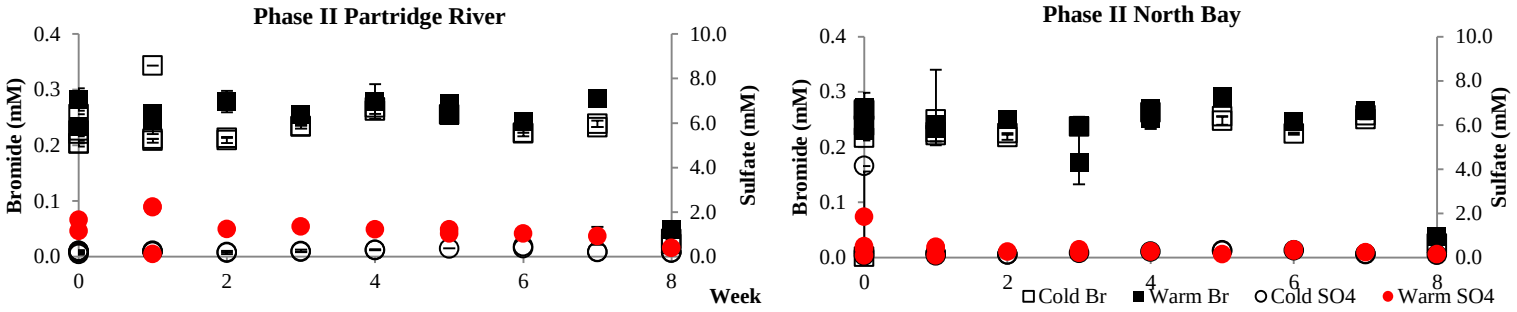

Figure 8 Overlying water concentrations of sulfate and bromide Left: Partridge River and Right: North Bay through Phase II. Multiple data points for one week indicate additional sampling during the week due to bromide or sulfate amendments. Filled symbols represent measurements made in 23°C microcosms and, hollow symbols represent measurements made in 4.5°C microcosms.

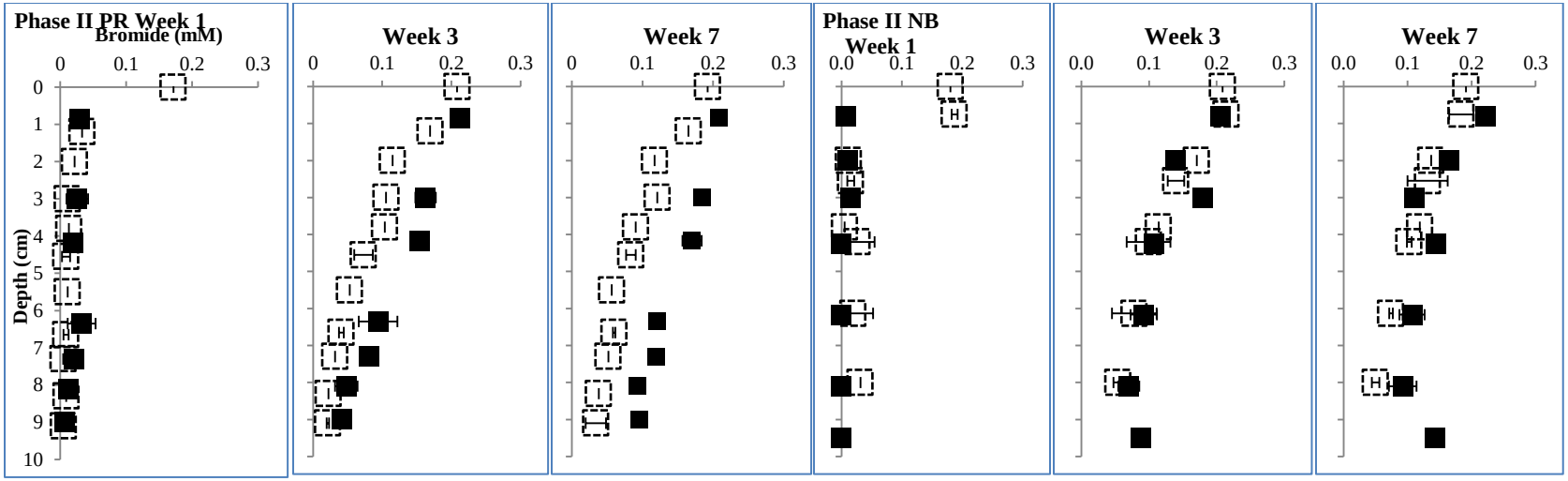

Figure 9 Porewater Bromide concentrations in warm and cold microcosms Left: Partridge River Right: North Bay. Filled symbols represent measurements made in 23°C Microcosms, hollow symbols represent measurements made in 4.5°C microcosms.

Relevance of lab measurements to field conditions

The characterization of porewater (during each experimental phase) and solid phase samples (beginning and end only) from the lab experiments provides a means of comparing laboratory measurements to field conditions. Sediment porosity was calculated from measured specific gravity and moisture content of the respective soils (wet basis, Appendix B). Porosity within the top 10 cm was very similar between *in situ* (avg. 74%) and laboratory settings (avg. 73%) for North Bay sediment. For PR, however, a significant difference in porosity was observed between in situ and lab conditions (avg. 91% in situ, avg. 80% lab) and was most likely due to sediment homogenization and consolidation at the beginning of the experiment. Variation in porosity between the experimental microcosms at the end of Phase I and Phase II was minor for NB (+/- 4%), and PR cold microcosms, but greater differences were noticed in-between the *in situ* and laboratory microcosms for Partridge River warm microcosms (laboratory microcosm porosity was 7% than *in situ*). A 10% difference was noticed between the warm and cold microcosms for Partridge River at the end of Phase II.

The difference in porosity between Partridge River and North Bay sediments can be attributed in part to the makeup of the sediments. Partridge River sediment had a higher organic content, higher porosity (Figures 13 & 17) and the specific gravity of the sediment solids was less dense ($\rho_s = 2.60$) compared to that of North Bay ($\rho_s = 2.62$). Overall, the unit weight of the Partridge River sediment was 2 kN m^{-3} less (16 kN m^{-3}) than then North Bay sediment (18 kN m^{-3}, Appendix B). Higher porosity in the Partridge River sediment would act to promote more rapid diffusion as the sediment matrix was less dense, and the tortuous path less encumbered. Higher porosity would also indicate the potential for a more rapid recovery once the upper boundary condition had changed. The North Bay sediment has lower porosity, which could restrict the movement of anions in solution, resisting rates of sulfate penetration and recovery (Figure 7). Sulfate trapped in the porewaters could have a greater potential to be reduced to sulfide as the sediment temperatures rise in spring and bacteria cultures become more active (Pallud & Van Cappellen, 2005).

pH measured during experiments differed little from in situ condition and varied only slightly throughout the experiment (cold microcosms approximately 7.1 and warm microcosms 6.9), most noticeably within the warm microcosms and may be reflective of the increased rates of chemical and biological processes taking place within the sediment similar to what was observed in Benjamin, 2002, (similar to *in situ* conditions, pH approximately 7.1; Figures 14 and 18).

The dissolved iron (II) concentrations measured during experiments deviated significantly from *in situ* conditions for both Partridge River (78% increase over the course of the experiment, avg. 526 µM-*in situ*, avg. 937 µM – end Phase II) and North Bay (606% increase over the course of the experiment, avg. 32 µM -*in situ*, avg. 226 µM – end Phase II) (Figures 15, 19) The differences between *in situ* and laboratory porewater iron (II) concentrations may have been due to the sediment disruptions that occurred during the transition into the microcosms. The difference may also have been caused by oxidation of Iron sulfides by Oxygen, Nitrate, Iron (III) or Manganese (IV). The electron acceptor becomes negatively charged and releases an oxygen molecule which readily binds with the sulfide to become sulfate (Schippers and Jorgensen, 2001). As the sediments were being homogenized for the experiment the disruption may have altered the predominant bacterial colonies within the sediment, and the observed changes in iron concentration may have been a result of bacteria colonies re-establishing themselves based on the altered geochemical environment (Figure 12, 16, 20). Since porewater iron concentrations in experimental microcosms were higher than in-situ observations, the porewater sulfide observed in response to sulfate loading and unloading is not representative of what may occur in a field setting.

Mass transport comparison of sulfate and bromide

Observed sulfate loss in overlying waters

Over the course of Phase I, the concentration of sulfate in the overlying water followed a downward trend in three of the four test treatments, allowing for an estimate of the total mass loss from the overlying water. Mass lost was calculated by summing the concentration decreases, multiplying the summations by the overlying water volume, and divided by cross sectional area of the microcosms to get a mass loss per unit area. The difference between the sulfate mass lost from the overlying water and what was present in the porewaters can be used to estimate biological consumption (Table 6).

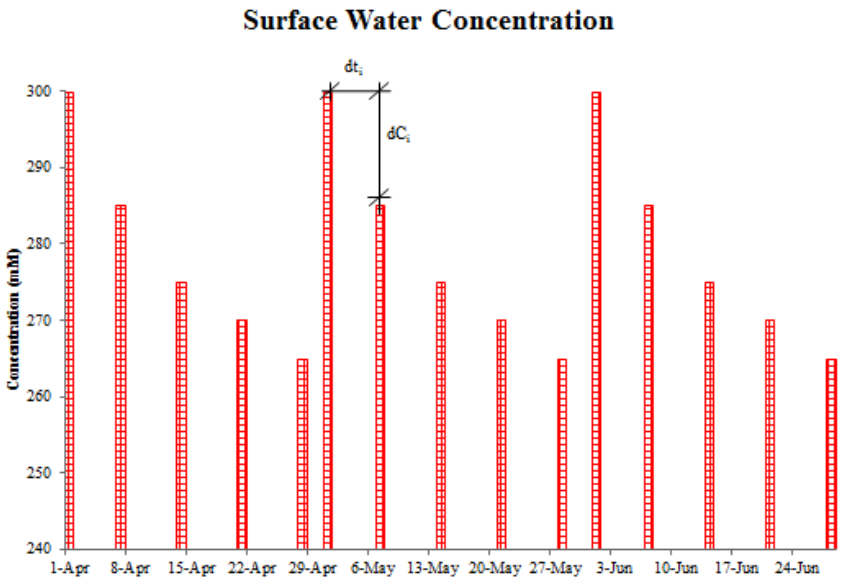

Figure 10 Visual example of summation of decrease in overlying water concentration (values do not correspond to actual measurements made during this experiment).

Overlying water mass loss

$$OWML = \sum_{i=1}^{n}(C_{ti} - C_{ti-1}) * \forall/(A) \quad \text{Eqn. 4}$$

OWML = overlying water mass loss$[mmole\ cm^{-2}]$
C_{ti}*= concentration at time t [µg/cm3]*
C_{i-1}*=concentration at previous time* t_{i-1} *[µg/cm3]*
$\forall$*=Volume of overlying water [cm]*
A=sediment surface area [cm2]

Assuming a conservative system in which total mass of the tracer ions remains constant throughout the experiment, the summation of mass lost from the overlying waters (Eqn. 4) should be accounted for by mass accumulation within the porewaters (Eqn. 5).Tracer mass accumulated in the porewater was calculated by assuming a curve on the depth-concentration plots, integrating the area underneath that curve, adjusting for depth dependent porosity, and subtracting off initial anion concentrations. In this way only the mass in excess of that present in the porewaters at the beginning of the respective phases was considered (Figure11, Eqn. 5; Tables 4-5).

Porewater mass accumulation

$$PWMA = \sum_{i=1}^{n} C_i * D_i \text{ Eqn. 5}$$

PWMA = Porewater mass accumulation$[mmole\ cm^{-2}]$
C_i=concentration at depth i [ug/cm3]
D_i=depth interval I [cm]

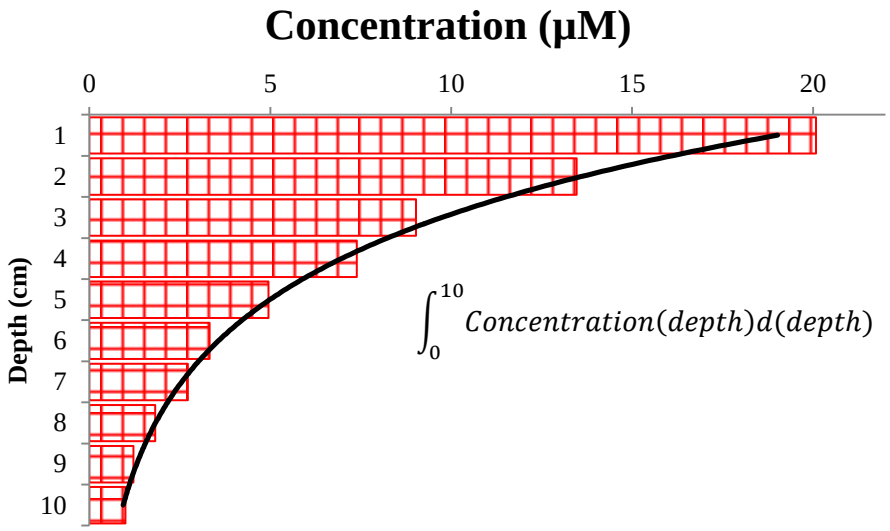

Figure 11 Example of integrating the area under the concentration-depth curve to obtain the mass accumulation within the porewaters. This is a visual representation, not representative of a particular set of measurements.

Bromide observations of PWMA results suggest slightly higher transport rates into the porewaters of the warm sediments when compared to the cold sediments (Table 4). Similar results were observed in the North Bay OWML calculations. Based on mathematical predictions and the results of this analysis, the hypothesis that diffusional transport occurs more quickly under warm conditions relative to cold conditions appears to hold true. The clouding of the overlying water and increases in sulfate observed in the warm Partridge River microcosms suggests that the overlying water may have been affected by processes other than diffusion and this may have compromised the OWML calculations for the Partridge River Microcosms. The more predictable trend of bromide penetration within the Partridge river warm microcosms seems to confirm that additional processes were affecting the transport of sulfate within the warm Partridge River sediment.

Table 4 Comparison of bromide mass lost from the overlying water and mass accumulation in the porewaters.

Bromide (20 days)	Partridge River Cold (mM m^{-2})	Partridge River Warm (mM m^{-2})	North Bay Cold (mM m^{-2})	North Bay Warm (mM m^{-2})
OWML	11. 6	7. 2	6. 8	12.0
PWMA	10. 2	12. 6	10. 1	11. 9

Estimates of the mass of sulfate reduced were made using a mass balance of sulfate losses in the overlying water and the sulfate accumulation in the porewater. Assuming a closed system, the difference between sulfate mass lost from the overlying water (averaged for each treatment) and sulfate mass gained (averaged for each treatment) in the porewater could only be accounted for by conversion to a form of sulfide. Measurements of dissolved sulfides in the porewaters and AVS samples taken of the sediment were not conclusive as to an appreciable rise in sediment sulfide, most likely due to the short duration of this experiment and comparison of a relatively small change to a large sulfide inventory. Slight increase in AVS within the cold Partridge River microcosms may have been present, but the variability of the data obscures a statistically significant difference (Figure 21). No discernable pattern was observed in the North Bay AVS measurements (Figure 22).

Estimates of instantaneous sulfate reduction rates were made using the Monod model (Equation 9). The Monod model with temperature adjusted observations of Pallud & Van Cappellen (2005)(Q_{10} = 2.4; Table 6) were used in conjunction with the measured porewater concentrations to predict sulfate reaction rates at the end of Phase I (Table 6; Eqn. 6), although actual rates in this sediment may differ from those observed by Pallud & Van Cappellen due to the organic carbon, iron, nitrate and other chemical contents of the sediment. The reaction rates estimated by the Monod equation fall on the low end of the range of the sulfate reaction rates measured for lakes (Bak and Pfenning, 1987). These rates cannot be confidently extrapolated to field conditions because of the variability in sediment geochemical and physical properties and other external factors such as ground water flow, bioturbation and temperature fluctuations.

Based on the mass balance calculations made from the laboratory observations of surface and porewater concentrations, and consistent with the hypothesis, sulfate reduction occurred faster in the warm North Bay sediments than the cold North Bay sediments (Table 6). Under the laboratory conditions reported here, a significant amount of sulfate was transformed to sulfide,

even at 4℃. 30% of the mass lost in the overlying water of the cold North Bay microcosm was accounted for in the porewaters, and sulfate mass was lost from the cold Partridge river sediments as well. The mass loss (overlying water) and porewater gain comparisons made in this study were consistent with the Monod reduction model based on the maximum reaction rate (R_{max}). Using the concentration at a particular depth (C_i), the half saturation constant (K_S) and the depth interval (D_i) (Eqn. 6, Table 6), sulfate reduction rates could be estimated based on the porewater measurements. Sulfate reduction estimates fall within the lower range of values measured by Bak and Pfenning (1987). A comparison of sulfate reduction based on a mass balance of overlying water mass loss and porewater accumulation could not be accurately made for the Partridge River sediments due to the unforeseen rise in overlying water sulfate concentration during the sulfate recovery phase and the high initial porewater sulfate concentrations in the cold Partridge River sediments. The Monod model was useful in obtaining estimates of the sulfate reduction within the top 10 cm of the sediment, there may have been other active biological communities competing with the sulfate reducers due to the high amounts of dissolved iron that became available as a result of the sediment disruption.

$$\sum_{i=1}^{n} \frac{R_{max} * C_i * D_i}{K_s + C_i} = Reduction\ rate$$ (Monod, 1949; Eqn. 6)

R_{max} = maximum reduction rate [mmol day^{-1} cm^{-2}]
C_i = concentration at depth$_i$ [mmol cm^{-3}]
D_i = depth interval$_i$ [cm]
K_s = reaction constant [mmol cm^{-3}]

Table 5 Sulfate mass balance estimated from mass lost from the overlying water and mass accumulations within the porewaters

Sulfate (64 days)	Partridge River 4.5°C	Partridge River 23°C	North Bay 4.5°C	North Bay 23°C
Overlying water Mass loss (mM m^{-2})	-134. 2	-16. 96	-230. 8	-305. 4
Porewater Mass accumulation (mM m^{-2})	-23. 42*	+131. 76	+73. 8	+82. 0

*negative mass accumulation in cold Partridge River sediments due to high initial porewater sulfate concentrations

Table 6 Sulfate reduction based on sulfate concentrations observed at the end of the sulfate loading phase and Sulfate reduction rates based on the Monod approximation

Sulfate (64 days)	Partridge River 4. 5°C	Partridge River 23°C	North Bay 4.5°C	North Bay 23°C
Cumulative sulfate Reduction (mM m^{-2}) *	-	-	157. 0	223. 4
Approximate sulfate reduction rate (mM m^{-2} day^{-1})$^{+}$	0. 51	3. 47	1. 86	2. 83

* Based on the difference between overlying water mass loss and porewater concentration increase.
$^{+}$Based on the Monod eqn. for sulfate reaction as a function of porewater concentrations

Table 7 Monod sulfate reaction parameters

Depth (cm)	**$R_{max\_23°C}$** **mM m^{-2} day^{-1}**	**$R_{max\_4.5°C}$** **mM m^{-2} day^{-1}**	**K_s** **mM**
0-2	16. 93	2. 58	0. 18
2-4	12. 65	1. 92	0. 11
4-6	4. 17	0. 63	0. 10
6-8	3. 98	0. 61	0. 15

R max Values were interpolated from Pallud and Cappellen (2005). Q10 values were used to adjuste tabulated Rmax values for the 4.5°C microcosms.

Conclusions and implications

Although sulfate is a naturally occurring form of sulfur and relatively benign in many situations, under certain conditions it can pose a threat to the health of wild rice and other aquatic vegetation. The state of Minnesota has taken this threat seriously and has sought to understand the mechanics behind sulfate's potentially damaging effects. In conjunction with the Minnesota Pollution Control Agency, this study has investigated the temperature dependence of sulfate transport under laboratory controlled conditions. Though both rates of sulfate diffusion and rates of sulfate reaction are known to depend on temperature (Baig & Hopton, 1969; Boudrea, 2003; Sinke et al., 1992), the net effect of these two temperature dependencies on the fate of sulfate and sulfide in sediments is not easily isolated. A thorough understanding of these processes is necessary to investigate the effectiveness of a complex loading phenomenon such as winter-only discharge of sulfate to overlying waters and the consequent implications for the chemistry of underlying sediments and pore waters. This study provided a temperature-dependent physical model to investigate the rates of sulfate transport and reaction in sediments that might occur in response to seasonal sulfate loading in the overlying water.

Two types of sediment, collected from the headwaters and estuary of the St. Louis River were incubated in experimental microcosms and subjected to loading and unloading of sulfate mass in the overlying water. The concentrations of sulfate and bromide (an inert tracer) in the overlying water were measured regularly to maintain a nearly constant upper boundary condition. Concentrations in the porewater were periodically sampled to monitor changes after key alterations to the overlying water. The measured concentrations were then compiled and analyzed to calculate the time dependent changes in sulfate and bromide concentrations both in the overlying water and sediment porewaters.

The laboratory experiment provided a simplified simulation of a diffusion controlled, natural system in an attempt to isolate the influence of temperature on sulfate transport into and out of sediment porewaters. Variables such as sediment disturbance, oxygen production via photosynthesis, and advective fluid movement were largely eliminated. As such, this experiment did not take into consideration effects of groundwater flow or seasonal temperature fluctuations that could be important in natural systems. This system did not explicitly seek to isolate the effects biological reaction from transport, but made inferences about the biological rates based on the observed sulfate concentrations in the overlying waters and sediment porewaters. Since the sediment used for the experiment came from natural systems, sediment-dwelling organisms presented an unforeseen variable in the sediment of the warm-temperature lab treatments. Though disturbances compromised the diffusion-only transport objectives of the experiment, the result showed that if a sediment disturbance was to occur in a natural system, the oxidation of the solid phase can mobilize a significant reservoir of sulfur (Sullivan et al., 1988: 'Iron sulfide').

Bromide provided an inert chemical tracer to analyze the influence of temperature on diffusion rates within two different types of sediment. Bromide mass lost from the overlying waters within the North Bay microcosms incubated under cold conditions was 56% of the mass lost from the overlying waters of the microcosms incubated under warm conditions, suggesting more rapid transport under warm conditions. With the exception of the warm Partridge River microcosms, bromide mass decreases observed in the overlying water was a good indicator of bromide mass increase in the porewaters, indicating the conservative nature of the bromide mass within the system (Table 4). Mass lost from overlying waters accounted for between 67 % and 113 % of the increased porewater mass after 20 days of bromide loading (Table 4).

Overlying water sulfate concentration measurements in the North Bay sediments over 64 days of sulfate loading indicate a decrease of 230.8 and 305.4 mM m^{-2} (cold and warm

respectively) and only a 73.8 and 82.0 mM m^{-2} (cold and warm respectively) gain in porewater sulfate (Table 5). This indicates that significant sulfate reduction occurred at both temperatures. The sulfate mass losses from the surface water throughout the first several weeks of the sulfate loading phase are indicative of the temperature dependence of the sulfate diffusion rates. Sulfate mass loss near the end of the sulfate loading phase was indicative of a situation in which diffusion rates matched reduction rates.

A greater amount of sulfate mass was lost from the surface water under the warm conditions compared to the cold. The sulfate mass accumulation within the porewaters is a complicated function of the diffusion from the overlying water, the geochemical makeup of the sediment, and the temperature dependent biological reduction within the sediment. After the first four weeks of the sulfate loading phase, the overlying sulfate concentration in the warm Partridge River microcosms began to rise. The rise in sulfate concentration within the warm microcosms combined with the elevated porewater sulfate levels at the beginning of the experiment in the cold microcosms compromised the effectiveness of a direct comparison between the two sediment sources. However, sulfate and bromide results from the North Bay sediments indicate that diffusion occurred more rapidly under warm conditions than cold. The results from a sulfate mass balance on the North Bay sediments indicated that less biological sulfate consumption occurred under cold conditions than warm conditions, which was consistent with the rates estimated using a temperature-dependent Monod model.

Sufficient quantities of sulfate in the overlying water can lead to appreciable transport into sediment, which can fundamental change the geochemical and biological processes that occur in freshwater anoxic aquatic sediments (Allam and Hollis, 1972; Koch and Medelssohn, 1989; Orem et al., 2011; Scheidt and Kalla, 2007). Elevated sulfate levels in the porewaters provide favorable conditions for sulfate reducing bacteria that, over time, could produce sulfide in excess of the available iron in a system and result in an accumulation of sulfide in pore fluids. Sufficient quantities of sulfide can be toxic to aquatic vegetation and organisms, and begin to affect the overlying waters as well. Apart from the results observed in the warm Partridge River microcosms, this study has demonstrated that lower temperatures decrease ionic diffusion within the sediment and sulfate reduction. Although this study was not sufficiently long enough to observe a statistically significant increase in the sediment sulfide content, the difference between the bromide results and the sulfate results indicates that the biological processes were indeed converting sulfate to sulfide, even at low temperatures. Though dependent on geochemistry of a

site, wild rice could be exposed to additional sulfide if cutoff dates for discharging elevated sulfate to overlying waters are not set sufficiently ahead of the sediment warming. As observed under the experimental conditions of this study, residual sulfate was still present in the cold sediments seven weeks after the sulfate loading had ended. Actual timing of sulfate residuals at field sites could differ from this due to more complex transport processes and site-specific geochemical conditions.

This study was conducted to observe the time and temperature dependent response to sulfate loading and unloading within the sediments of the St. Louis River watershed. Although it is not an exhaustive study of sulfate diffusion, it presents the observed response of sediment porewaters to an increase and decrease in overlying water sulfate concentration under laboratory controlled and diffusion dominated conditions. From a transport perspective, diffusion processes occur more rapidly under warmer conditions. Diffusion of bromide and sulfate from the overlying water proceeded at a higher rate under warm conditions than they did at colder conditions. From a biological standpoint, sulfate reduction rates decreased with decreasing temperatures. From the standpoint of defining rooting zone geochemistry relevant to wild rice, sulfate has less potential to be converted to sulfide under cold environmental conditions than it has under warm environmental conditions, but this slower conversion to sulfide causes sulfate to remain elevated in porewaters for a longer time after surface water loading ceases.

Future Studies

Though porewater sulfide was measured initially and at the end of each phase, no quantifiable change in dissolved sulfide was observed over the course of the nine-month study. A similar, 21-month study conducted by Van der Welle et al. 2007 in a peat meadow observed a strong negative relationship between iron and sulfide concentrations within sediment porewaters. Based on the geochemistry of the sediments used for the study described herein, where high iron concentrations were observed, low sulfide concentrations could be expected based on the formation of insoluble iron sulfide compounds. Our hypothesis was that a decrease in porewater iron might be observed during the loading phase of the study as iron sulfide was formed. However, the sulfate exposure portion of this study was not long enough to allow the titration of the high iron content (including solid phase) of the sediment and an appreciable accumulation sulfide in the porewaters. A related study conducted in field mesocosms observed appreciable increases in porewater sulfide and decreases in porewater iron over the course of 3 years of continuous 300 mg/L overlying water amendments (Johnson, 2014). It would be of interest to

lengthen the sulfate-loading phase, or possibly conduct the experiment with sediments low in iron content to observe the long-term effects of sulfate loading and accumulation of sulfides within the sediment.

Within this study the overlying water was constantly bubbled, both to keep the water aerated as well as provide mixing in the water. It would be interesting to conduct this study with continuously flowing water, to better simulate a riverine scenario. A flow-through system would also be more effective at maintaining a constant overlying water sulfate concentration, as the concentration would not fluctuate based on the amount of sulfate diffusion that had occurred, and the overlying water concentration would also be consistent between the replicates. A flow-through system was not utilized during this study because of the objective to monitor the individual sulfate mass balance between the overlying water and porewaters. After seeing the consistency between the individual microcosms, a flow-through system would provide a more efficient means of maintaining a consistent overlying water concentration.

This study utilized two types of sediment retrieved from the St. Louis River watershed, both of which were comprised of silt-like material. These sediments provided a small sample of two types of sediment (disturbed) found within the St. Louis River watershed, however a similar analysis would be interesting for a more sand-like material. The geochemical and physical make up of sandier sediment would provide an interesting contrast to the previously utilized sediments as the organic content of sandy sediment as well as the porosity could significantly impact both sulfate transport and reduction rates.

The system designed for this study provided a simplified representation of temperature dependent diffusion as it occurs within natural systems. By using the observations obtained from this study, a mathematical model could be constructed and calibrated to estimate the temperature-dependence of sulfate diffusion and reaction. As a part of future studies, the temperature dependence of sulfate diffusion and reaction could be utilized in scenarios with higher complexity to assist managing agencies in decisions about sulfate release, release cutoff dates, and best management practices.

References

Allam, A. I., & Hollis, J. P. (1972). Sulfide inhibition of oxidases in rice roots. *Phytopathology* (*62*): 634-639.

Armstrong, J., Armstrong, W. (2005) Rice: Sulfide-induced Barriers to Root Radial Oxygen Loss, Fe2+ and Water Uptake, and Lateral Root Emergence. Annals of Botany (96):625-638.

ASTM D 854-10: Standard test for specific gravity of soil solids by water in a volumetric flask

ASTM D 2216-10 Standard Methods for Laboratory determination moisture Content of Soil and Rock by mass method.

Azzoni, R., Giordani, G., & Viaroli, P. (2005). Iron-sulphur-phosphorus interactions: implications for sediment buffering capacity in a mediterraneaneurophic lagoon (sacca di goro, Italy). *Hydrobiologia* (550): 131-148.

Bak, F., Pfenning, N. (1991) Microbial sulfate reduction in littoral sediment of Lake Constance. *FEMS Microbiology Ecology* 85: 31-42.

Benjamin, M. (2002). *Water chemistry*, Long Grove, IL: Waveland Press, Inc.(1) : 333.

Berndt, M., & Bavin, T. Minnesota Department of Natural Resources (2012). *On the cycling of sulfur and mercury in the St. Louis river watershed, northern Minnesota*.

Berndt, M., & Bavin, T. Minnesota Dept. of Natural Resources, Division of Lands and Minerals. (2009) *Sulfate and mercury chemistry of the St. louis river in northeastern Minnesota*.

Berner, R. A. (1970). *Sedimentary pyrite formation*. Informally published manuscript, Department of Geology and Geophysics, Yale University, New Haven, CT,

Baig, I. A., & Hopton, J. W. (1969). *Phychrophilic properties and the temperature characteristic of growth of bacteria* 100: 552-553.

Boudreau, B. P. (2003). *Diagenetic models and their implementation, modelling transport and reactions in aquatic sediments*. (1st ed.). New York, NY: Springer.

Caliman, A., J. J. F. Leal, F. A. Esteves, L. S. Carneiro, R. L. Bozelli, and V. F. Farjalla. (2007). Functional bioturbator diversity enhances benthic–pelagic processes and properties in experimental microcosms. *Journal of the North American Benthological Society* 26:450–459.

Cook, R. B., Schindler, D. W. (1983) The Biogeochemistry of sulfur in an experimental acidified lake. *Environmental Biogeochemistry*. Ecology Bulletin, Stockholm. 35 :115-127

Covich, A. P., M. C. Austen, F. Bärlocher, E. Chauvet, B. J. Cardinale, C. L. Biles, P. Inchausti, O. Dangles, M. Solan, M. O. Gessner, B. Statzner, and B. Moss. (2004). The role of biodiversity in the functioning of freshwater and marine benthic ecosystems. *Bio-Science* 54:767–775.

De Jonge, M., Teuchies, J., Meire, P., Blust, R., Bervoets, L. (2012) The impact of increased oxygen conditions on metal contaminated sediments part 1: Effects on redox status, sediment geochemistry and metal bio-availability. *Water Research.* 46(7):2205-2214

de Wit, R., Stal, L. J., Lomstein, B. Aa., Herbert, R. A., Gemerden, H., Viaroli, P., Ceccherelli, V. U., Radriqez-Valera, F., Bartoli, M., Giordani, G., Azzoni, R., Shaub, B., Welsh, D. T., Donnely, A., Cifuentes, A., Anton, J., Finster, K., Nielsen, L. B., Underlien Pedersen, A. G., Neubauer, A. T., Colangelo, M. A., Heijs, S. K., (2001). ROBUST: The Role of Buffering capacities in stabilizing coastal lagoon ecosystems. *Continental Shelf Research* (21): 2021-2041.

Eaton, A., Clesceri, E., Rice, E., & Greenberg, A. (Eds. 2005), 3500-Fe-B Phenanthroline Method. In *Standard Methods for the examination of water and wastewater* (21 ed.). Baltimore, Maryland: Port

Eaton, A., Clesceri, E., Rice, E., & Greenberg, A. (Eds. 2005), 4500-S^{2-} D. Methylene Blue Method. In, *Standard Methods for the examination of water and wastewater* (21 ed.). Baltimore, Maryland: Port

Eaton, A., Clesceri, E., Rice, E., & Greenberg, A. (Eds. 2005), 4110 C. Single Column Ion Chromatography., *Standard Methods for the examination of water and wastewater* (21 ed.). Baltimore, Maryland:

Port Fossing, H., Ferdelman,T. G., Berg, P. (2000) Sulfate reduction and methane oxidation in continental margin sediments influenced by irrigation (South-East Atlantic off Namibia), Geochim. Cosmochim. Acta 64 (5): 897–910.

Fossing, H., Ferdelman, T.G., and Berg., P. (2000). Sulfate reduction and methane oxidation in continental margin sediments influenced by irrigation (South – East Atlantic off Namibia). Geochim. Cosmochim. Acta 64 (5): 897-910

Gao, S., Tanji, K., & Scardaci, S. (2003). Incorporating straw may induce sulfide toxicity in paddy rice. *California Agriculture:* 55-59.

Gerino, M., G. Stora, F. François-Carcaillet, F. Gilbert, J-C. Poggiale, F. Mermillod-Blondin, G. Desrosiers, and P. Vervier. (2003). Macro-invertebrate functional groups in freshwater and marine sediments: a common mechanistic classification. *Vie et Milieu* 53:221–232.

Gilmour, C., Roden, E., & Harris, R. (2007) Approaches to modeling sulfate reduction and methymercury production in the everglades. *The South Florida environment, 1*.

Giordani, G., Bartoli, M., Cattadori, M., Viaroli, P., (1996). Sulfide release from anoxic sediments in relation to iron availability and organic matter recalcitrance and its effects on inorganic phosphorus recycling. *Hydrobiologia.*(329): 211-222.

Heijs, S. K., Gemerden, H., (2000). Microbial and environmental variables involved in the sulfide buffering capacity along a eutrophication gradient in a coastal lagoon (Bassind'Archachon, France). *Hydrobiologia* (437): 121-13.

Heijs, S., Jonkers, H., Gemerden, H. v., Schaub, B., & Stal, L. (1999) The Buffering Capacity Towards Free Sulfide in Sediments of a Coastal Lagoon (Bassin d'Arcachon, France) - The Relative Importance of Chemical and Biological Processes. *Estuarine, Coastal and Shelf Science. 49*: 21-35.

Holmer, M., & Storkholm, P. (2001). Sulphate reduction and sulphur cycling in lake sediments: a review. *Freshwater Biology 46*: 431-451.

Ingvorsen, K., Zeikus, J. G., Brock, T. D. (1981) Dynamics of bacteria sulfate reduction in a eutrophic lake. *Applied Environmental Microbiology:* 1029-1036.

Iversen, N., & JØrgensen, B. (1992). Diffusion coefficients of sulfate and methane in marine sediments: influence of porosity. *Geochimica Acta 57*: 571-578.

Johnson, N. W. (2014) Response of rooting zone geochemistry to experimental manipulation of sulfate levels in wild rice mesocosms. MPCA Report. February 2014.

Koch, M. S., Mendelssohn, I. A. (1990) Sulphide as a soil phytotoxin: Differential responses in two marsh species. *Journal of Ecology* 77: 565-578.

Kristensen, E. (2000). Organic matter diagenesis at the oxic/anoxic interface in coastal marine sediments, with emphasis on the role of burrowing animals. *Hydrobiologia* 426:1–24.

Koschorreck, M., & Wendt-Potthoff, K. (2012). A sediment exchange experiment to assess the limiting factors of microbial sulfate reduction in acidic mine pit lakes. Journal of *Soils Sediments 12*:1615-1622.

Küsel, K., Roth, U., Trinkwalter, T., Peiffer, S., (2001), Effect of pH on the anaerobic microbial cycling of sulfur in mining-impacted freshwater lake sediments. *Environ Exp*. Bot 46: 213-223.

Lewandowski, J., C. Laskov, and M. Hupfer. (2007). The relationship between *Chironomus plumosus* burrows and the spatial distribution of pore-water phosphate, iron and ammonium in lake sediments. *Freshwater Biology* 52:331–343.

Lovley, D. R., Klug M. J. (1983), Sulfate reducers can outcompete methanogens at freshwater sulfate concentrations. *Applied Environmental Microbiology* 45:187-192.

Lovley, D. R., Klug M. J. (1985), Model for the distribution of sulfate reduction and methanogenesis in freshwater sediments. *Geochimica et Cosmochimica Acta* 50:11-18.

Mermillod-Blondin, F. and R. Rosenberg. (2006). Ecosystem engineering: the impact of bioturbation on biogeochemical processes in marine and freshwater benthic habitats. *Aquatic Sciences* 68:434–442.

Mermillod-Blondin, F. (2011). The functional significance of bioturbuation and biodeposition on biogeochemical processes at the water-sediment interface in freshwater and marine ecosystems. *Journal of the North American Benthological Society 30*(3): 770-778.
Minnesota Pollution Control Agency, (2013). *Minnesota's sulfate standard to protect wild rice*. Minnesota Pollution Control Agency, Environmental Outcomes Division. (1999). *Sulfate in Minnesota's ground water*.
Molongoski, J. J., Klug, M. J. (1980) Anaerobic metabolism of particulate organic matter in the sediments of a hypereutrophic Lake. *Freshwater Biology* 10: 507-518.
Monod, J. (1949). The growth of bacterial cultures. *Annual Review of Microbiology*. 3: 371-394.
Moyle, J. (1944) Wild Rice in Minnesota. *Journal of Wildlife Management 8*: 177-184.
Orem, W., (2007). Sulfur contamination in the Florida everglades: Initial examination of mitigation strategies: U.S. Geological Survey Open-Files Report 2007-1374.
Orem, W., Gilmour, C., Axelrad, D., Krabbenhoft, D., Scheidt, D., Kalla, P., McCormick, P., & Gabriel, M. (2011). Sulfur in the south Florida ecosystem: Distribution, sources, biogeochemistry, impacts and management for restoration. *Critical Reviews in Environmental Science and Technology*. *41*(6): 249-288.
Pallud, C., and Van Cappellen, P. (2006). *Kinetics of microbial sulfate reduction in estuarine sediments*. Geochimica Cosmchimical Acta 70:1148-1162.
Palmer, M. A., A. P. Covich, B. J. Finlay, J. Gilbert, K. D. Hyde, R. K. Johnson, T. Kairesala, P. S. Lake, C. R. Lovell, R. J. Naiman, C. Ricci, F. F. Sabater, and D. L. Strayer. (1997). Biodiversity and ecosystem processes in freshwater sediments. *Ambio* 26:571–577.
Raiswell, R., & Canfield, D. E. (1998). Sources of iron for pyrite formation in marine sediments. *American Journal of Science 298*: 219-245.
Robinson, R., & Stotes, R. (1959). *Electrolyte solutions*. New York: Academic Press.
Rozan, T. F., Taillefert, M., Trouwborst, R. E., Glazer, B. T., Ma, S., Herszage, J., , Valdes L. M., Price, K. S., Luther, G. W III., (2002). Iron-sulphur-phosphorus cycling in the sediments of a shallow coastal bay: Implications for sediment nutrient release and benthic macroalgal blooms. *Limnology and Oceanography* (47): 1346-1354.
Sass, H., Cypionka, H., Babenzien, H. D. (1997) Vertical distribution of sulfate-reducing bacteria at the oxic-anoxic interface in sediments of the oligotrophic lake Stechlin. *FEMS Microbiology Ecology* 22: 245-255.
Scheidt, D.J., and P.I. Kalla., (2007). Everglades ecosystem assessment: water management and quality, eutrophication, mercury contamination, soils and habitat: monitoring for adaptive management: a R-EMAP status report. USEPA Region 4, Athens, GA. EPA 904-R-07-001: 98.
Schippers, A., & Jorgensen, B. B. Biogeochemistry of Pyrite and Iron Sulfide oxidation in Marine Sediments. *Geochimica et Cosmochimica Acta 66*: 85-92.
Seeberg-Elverfeld, J., Schluter, M., Feseker, T., & Kolling, M. (2005). Rhizon sampling of porewaters near the sediment-water interface of aquatic systems. Limnology and oceanography: Methods, 3. 361-371.
Sinke, A. J. C., Cornelese, A. A., Cappenberg, T. E., Zehnder, A. J. B. (1992) Seasonal variation in sulfate reduction and methanogenesis in peaty sediments of eutrophic Lake Loosdrecht, The Netherlands. *Biogeochemistry* 16: 43-61.
Smith, R. L., Klug, M. J. (1981) Reduction of sulfur compounds in the sediments of a eutrophic lake basin. *Applied Environmental Microbiology* 41: 1230-1237.
Smolders, A., Lamers, L., Hartog, C., & Roelofs, J. (2003). Mechanisms involved in the decline of Stratiotes aloides L. in The Netherlands: Sulphate as a key variable. *Hydrobiologia*, 603-610.
Spears, G. (2005). Sulfate. *Dietary Reference Intakes for Water, Potassium, Sodium, Chloride, and Sulfate*. Washington, D. C.: National Academies Press.

Stal, L., Behrens, S. B.,Vilbrant, M., van Bergeijk, S., Kruying, F., (1996). The biogeochemistry of two eutrophic marine lagoons and its effects on microphytobenthic communities. *Hydrobiologia* (329): 185-198.

Steenbergen, C. L. M., Sweerts, J. P. R. A., Cappenberg, T. E. (1993) Microbial biogeochemical activities in lakes: stratification and eutrophication. *Aquatic Microbiology: an Ecological Approach.* (Ed. T. E. Ford) Oxford. Blackwell Scientific Publications: 69-99.

Sullivan, P. J., Reddy, K. J., & Yelton, J. L. (1988). Iron sulfide oxidation and the chemistry of acid generation. *Environmental Geological Water Science, 11*(3): 289-295.

Urban, N., Sampson, C., Brezonik, P., & Baker, L. Sulfur cycling in the water column of Little Rock Lake, Wisconsin. *Biogeochemistry*: 41-77.

Van Der Welle, M. E. W., Smolders, A. J. P., Op Den Camp, H. J. M., Roelofs, J. G. M., & Lamers, L. P. M. (2007). Biogeochemical interactions between iron and sulfate in freshwater wetlands and their implications for interspecific competition between aquatic macrophytes. *Freshwater Biology 52*: 434-447.

Yuan-Hui, L., & Gregory, S. (1973) Diffusion of ions in sea water and in deep sea sediments. *Geochimica et Cosmochimica Acta 38*: 703-1714.

White, P. A., Kalff, J., Rasmussen, J. B., & Gasol, J. M. (1990). The effect of temperature and algal biomass on bacterial production and specific growth rate in freshwater and marine habitats. *Microbial Ecology* (21): 99-118.

Appendix A.

Table 8 Outline of experimental schedule with dates of important experimental considerations, anion amendment, overlying water replacement and porewater sampling. Weeks indicate full 7 day periods since the beginning of the phase

Phase	Week (dates)	Anion Spike	Water Replacement	Overlying water samples	Porewater sampling
Equilibrium	0 (2/20)			2/20	
	1 (2/25)			2/27	
	2 (3/4)		3/8PR	3/5	
	3 (3/11)			3/11	3/12,3/15
	4 (3/17)		3/20 PR	3/19	
	5 (3/25)			3/26	
	6 (4/1)			4/2	4/9-4/10
	7 (4/8)			4/8	
	8 (4/15)		4/15	4/15	
	9 (4/22)			4/22	
I Sulfate (SO_4^-)	0 (4/22)	4/23		4/24	
	1 (4/29)		4/29 PR	4/30	4/30
	2 (5/6)			5/7	
	3 (5/13)	5/17		5/13	
	4 (5/20)	5/23		5/20	
	5 (5/27)			5/28	
	6 (6/3)			6/3	6/4
	7 (6/10)			6/10	
	8 (6/17)			6/17	
	9 (6/24)	6/28*	6/28	6/26,6/28	6/25
	10 (7/1)				
	11 (7/8)		7/9	7/8,7/9,7/12	
II Bromide (Br^-)	0 (7/15)	7/15,7/17	7/17	7/15,7/17	7/16
	1 (7/22)	7/24	7/24	7/24,7/24,7/28	
	2 (7/29)	7/29	7/29		
	3 (8/5)			8/5	8/5
	4 (8/12)			8/12	
	5 (8/19)	8/21	8/21 PR	8/20	
	6 (8/26)			8/29	
	7 (9/2)			9/6	9/5
	8 (9/9)			9/9	

Overlying water concentrations

Table 9 Overlying water sulfate concentrations, Partridge River

days	date	4. 5C (mg/L)	23C (mg/L)	dMass Cold	Mass Warm	Σδmass Cold	Σδmass Warm
	20-Feb	230. 3	283. 4				
	27-Feb	52. 3	64. 6	-536. 9	-660. 1		
	5-Mar	280. 1	341. 7	687. 1	836. 2		
	11-Mar	105. 8	106. 9	-525. 8	-708. 6		
	19-Mar	121. 1	108. 9	46. 1	6. 0		
	26-Mar	90. 5	76. 6	-92. 3	-97. 3		
	2-Apr	102. 2	80. 9	35. 3	13. 0		
	8-Apr	110. 7	84. 2	25. 6	10. 0		
	15-Apr	115. 4	84. 7	14. 4	1. 3		
0	22-Apr	78. 8	74. 9	-110. 5	-29. 5		
2	24-Apr	291. 9	298. 2	-24. 4	-5. 5	-24. 4	-5. 5
8	30-Apr	276. 9	275. 8	-45. 2	-67. 6	-69. 6	-73. 1
15	7-May	257. 9	270. 4	-57. 4	-16. 4	-127. 0	-89. 4
21	13-May	244. 5	272. 9	-40. 5		-167. 5	-89. 4
28	20-May	297. 3	355. 2			-167. 5	-89. 4
36	28-May	293. 9	385. 9	-10. 1		-177. 6	-89. 4
42	3-Jun	287. 4	436. 7	-19. 5		-197. 1	-89. 4
49	10-Jun	234. 1	397. 3	-161. 0	-119. 1	-358. 2	-208. 6
56	17-Jun	223. 8	450. 1	-30. 9	159. 4	-389. 0	-49. 2
65	26-Jun	287. 3	660. 6			-389. 0	-49. 2
67	28-Jun	364. 9	395. 0			-389. 0	-49. 2
77	8-Jul	364. 8	641. 8	-0. 4		-389. 4	-49. 2
78	9-Jul	34. 8	56. 5				
81	12-Jul	54. 9	156. 7	60. 7	302. 3	60. 7	302. 3
84	15-Jul	21. 7	111. 8	31. 6	303. 3	92. 2	605. 6
86	17-Jul	25. 9	159. 8	12. 6	144. 9	104. 8	750. 5
93	24-Jul	25. 9	213. 9	45. 3	163. 3	150. 1	913. 7
97	28-Jul	17. 6	119. 1	21. 3	327. 4	171. 3	1241. 2
105	5-Aug	24. 8	130. 6	21. 6	34. 7	192. 9	1275. 8
112	12-Aug	30. 1	117. 8	16. 2	305. 2	209. 1	1581. 1
120	20-Aug	36. 0	99. 9	17. 9	249. 7	227. 0	1830. 8
129	29-Aug	37. 4	100. 5	4. 2	1. 8	231. 2	1832. 6
137	6-Sep	21. 7	89. 9	-47. 5	-32. 1		
140	9-Sep	17. 3	38. 3	-13. 3	-155. 6		
Σδmass (phase I Week 9)(mg/cm^3)						-389. 0	-49. 2
Σδmass/area (phase I Week 9)(mg/cm^2)						-134. 23	-16. 96
Σδmass (phase II Week 9)(mg/cm^3)						231. 2	1832. 6
Σδmass/area (phase II Week 9)(mg/cm^2)						79. 76	632. 33

Table 10 Overlying water sulfate concentrations, North Bay

days		4. 5C (mg/L)	23C (mg/L)	dmass Cold	dmass Warm	Σδmass Cold	Σδmass Warm
	20-Feb	19. 4	22. 1				
	27-Feb	23. 4	23. 0	12. 1	2. 7		
	5-Mar	25. 0	25. 4	4. 7	7. 4		
	11-Mar	26. 8	26. 9	5. 6	4. 5		
	19-Mar	27. 1	29. 8	0. 9	8. 8		
	26-Mar	29. 0	32. 8	5. 6	8. 8		
	2-Apr	30. 5	38. 6	4. 8	17. 6		
	8-Apr	31. 9	41. 9	4. 0	10. 1		
	15-Apr	31. 3	44. 3	-1. 8	7. 1		
0	22-Apr	17. 3	22. 8	-42. 1	-64. 7		
2	24-Apr	277. 4	274. 3	-68. 2	-77. 4	-68. 2	-77. 4
8	30-Apr	255. 7	262. 3	-65. 4	-36. 3	-133. 6	-113. 8
15	7-May	166. 5	80. 0	-269. 2	-550. 1	-402. 8	-663. 8
21	13-May	212. 3	236. 5			-402. 8	-663. 8
28	20-May	303. 2	320. 0			-402. 8	-663. 8
36	28-May	288. 5	312. 8	-44. 4	-21. 8	-447. 2	-685. 7
42	3-Jun	288. 8	321. 1			-447. 2	-685. 7
49	10-Jun	215. 3	255. 0	-221. 6	-199. 4	-668. 8	-885. 1
56	17-Jun	214. 4	263. 2			-668. 8	-885. 1
65	26-Jun	267. 0	344. 9			-668. 8	-885. 1
67	28-Jun	349. 8	320. 2			-668. 8	-885. 1
77	8-Jul	336. 0	365. 7			-668. 8	-885. 1
78	9-Jul	21. 8	25. 3				
81	12-Jul	37. 0	61. 8	45. 8	110. 2	45. 8	110. 2
84	15-Jul	22. 5	39. 7	25. 4	77. 2		187. 4
86	17-Jul	25. 0	49. 1	7. 4	28. 3	53. 3	215. 7
93	24-Jul	19. 7	43. 8	36. 1	108. 8		324. 5
97	28-Jul	13. 2	25. 1	14. 6	50. 8		375. 3
105	5-Aug	19. 6	19. 5	19. 4		72. 7	
112	12-Aug	25. 1	26. 2	16. 6	20. 3	81. 8	395. 6
120	20-Aug	28. 1	14. 0	9. 1		90. 9	
129	29-Aug	30. 9	29. 2	8. 3	45. 9	99. 2	441. 5
137	6-Sep	15. 2	22. 2				
140	9-Sep	11. 3	13. 7				
Σδmass (phase I Week 9)						-668. 8	-885. 1
Σδmass/area (phase I Week 9) (mM/m^2)						-230. 8	-305. 4
Σδmass (phase II Week 9)(mg/cm^3)						99. 2	441. 5
Σδmass/area (phase II Week 9)(mM/m^2)						34. 2	152. 3

Porewater concentrations

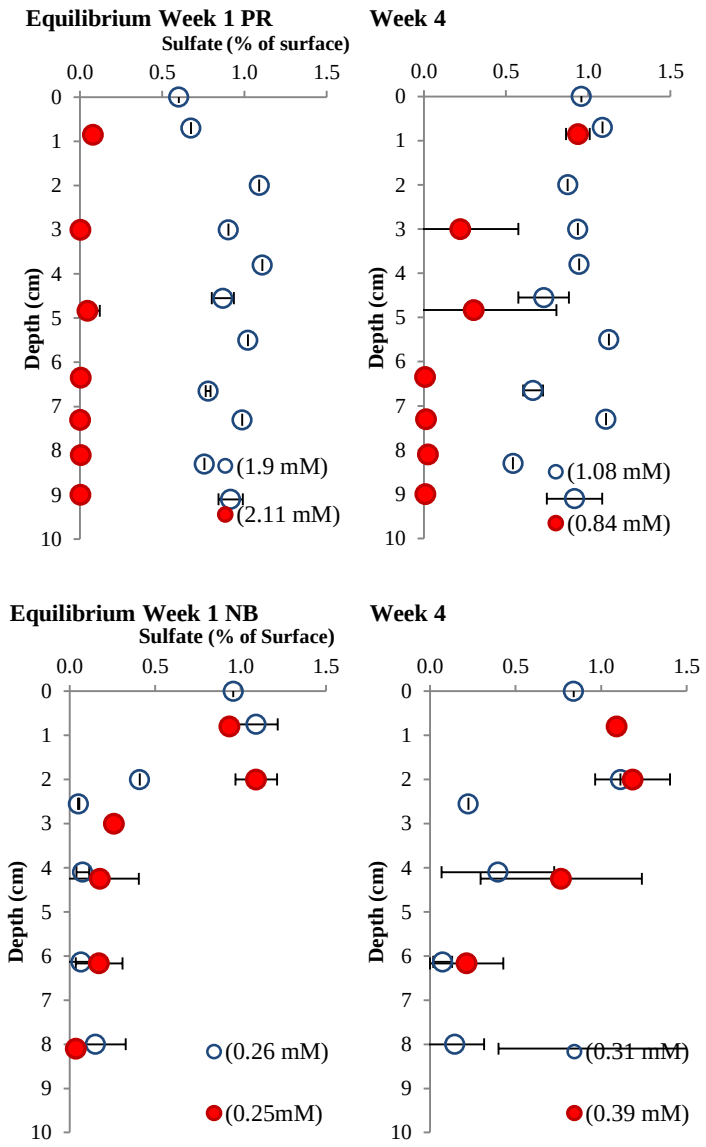

Figure 12 Porewater sulfate concentrations during equilibrium phase (Top Left) Partridge River Week 1 (Top Right) Partridge River Week 4 (Bottom Left) North Bay Week 1 (Bottom Right) North Bay Week 4. Filled symbols indicate 23°C microcosms, open symbols indicate 4.5°C microcosms.

Table 11 PR Cold porewater Sulfate concentrations*

Phase	Overlying Concentration	Depth below SW interface	9. 1	8. 3	7. 3	6. 7	5. 5	4. 6	3. 8	3. 0	2. 0	0.7	0.0
EQ 3	(1. 9 mM)	11-Mar	1.74	1.44	1.87	1.48	1.94	1.65	2.11	1.72	2.07	1.28	1.14
EQ 3	(0. 01 mM)	15-Mar	1.69	1.37	1.89	1.49	2.00	1.61	1.89	1.77	1.99	1.42	1.47
EQ 7	(1. 08 mM)	9-Apr	0.99	0.59	1.20	0.72	1.22	0.79	1.02	1.01	0.94	1.17	1.03
PH1-1	(2. 96 mM)	30-Apr	0.59	0.23	0.78	0.39	0.79	0.53	1.10	1.05	1.22	2.80	2.89
PH1-6	(3. 05 mM)	4-Jun	0.30	0.11	0.45	0.40	0.58	0.79	1.12	1.25	0.81	2.31	2.08
PH1-9	(2. 33 mM)	25-Jun	0.11	0.08	0.32	0.34	0.49	0.77	0.87	1.31	0.96	1.68	1.87
PH2-0	(0. 86 mM)	16-Jul	0.21	0.18	0.60	0.46	0.82	1.02	1.41	1.71	1.09	0.55	0.30
PH2-3	(0. 23 mM)	5-Aug	0.11	0.08	0.34	0.27	0.52	0.48	0.59	0.80	0.37	0.34	0.26
PH2-7	(0. 36 mM)	5-Sep	0.01	-	0.04	0.00	0.02	0.15	0.23	0.20	-	-	-

Table 12 PR Warm porewater Sulfate concentrations*

Phase	Overlying Concentration	Depth below SW interface	10. 5	9. 0	8. 1	7. 3	6. 4	4. 8	3. 0	0. 9
EQ 3	(2. 11 mM)	11-Mar	0.0	0.0	0.0	0.0	0.0	0.1	0.0	0.2
EQ 3	(0. 01mM)	15-Mar	0.0	0.0	0.0	0.0	0.0	0.0	0.0	0.0
EQ 7	(0. 84 mM)	9-Apr	0.0	0.0	0.0	0.0	0.0	0.3	0.2	0.8
PH1-1	(3. 09 mM)	30-Apr	0.0	-	0.0	0.0	0.0	0.1	1.0	2.7
PH1-6	(4. 28 mM)	4-Jun	0.0	0.0	0.0	0.0	0.1	0.6	1.9	3.0
PH1-9	(4. 69 mM)	25-Jun	-	0.6	0.0	0.0	0.9	0.8	2.5	3.6
PH2-0	(2. 52 mM)	16-Jul	0.0	0.0	0.0	0.2	0.5	1.1	2.1	1.9
PH2-3	(0. 91 mM)	5-Aug	-	-	0.0	0.0	0.1	0.2	0.5	1.2
PH2-7	(1. 06 mM)	5-Sep	0.0	-	0.0	0.0	0.0	0.0	0.3	0.5

Table 13 North Bay Cold porewater sulfate concentrations*

Phase	Overlying Concentration	Depth below SW interface	8.0	6.1	4.1	2.6	2.0	0.8	0
EQ 3	(0. 26 mM)	12-Mar	0.0	0.0	0.0	0.0	0.1	0.3	0.2
EQ 3	(0. 25mM)	15-Mar	0.0	0.0	0.0	0.0	0.0	0.0	0.0
EQ 7	(0. 31 mM)	10-Apr	0.0	0.0	0.1	0.1	0.3	0.7	0.3
PH1-1	(2. 93 mM)	30-Apr	0.8	0.3	0.4	0.6	1.0	2.4	2.7
PH1-6	(3. 00 mM)	4-Jun	0.7	0.6	1.1	1.4	1.6	2.1	2.0
PH1-9	(2. 55 mM)	25-Jun	-	0.8	1.1	1.4	1.7	2.0	1.9
PH2-0	(1. 46 mM)	16-Jul	0.3	0.7	1.4	1.8	1.8	0.3	0.3
PH2-3	(0. 16 mM)	5-Aug	0.6	0.7	0.9	0.8	0.8	0.3	0.3
PH2-7	(0. 25 mM)	5-Sep	0.0	0.1	0.5	0.3	0.4	0.0	-

Table 14 North Bay Warm porewater sulfate concentrations*

Phase	Overlying Concentration	Depth below SW interface	10. 4	9. 5	8. 1	6.17	4. 3	3	2	0. 8
EQ 3	(0. 25mM)	12-Mar	0.01	0.01	0.01	0.04	0.04	0.07	0.28	0.24
EQ 3	(0. 25mM)	15-Mar	0.01	0.01	0.00	0.03	0.04	0.00	0.10	0.23
EQ 7	(0. 39 mM)	10-Apr	0.01	0.22	0.72	0.08	0.30	0.60	0.46	0.43
PH1-1	(2. 73 mM)	30-Apr	0.00	0.00	0.01	0.14	0.18	0.98	1.66	2.18
PH1-6	(3. 37 mM)	4-Jun	0.00	0.00	0.01	0.10	0.42	1.11	1.60	1.87
PH1-9	(2. 84 mM)	25-Jun	-	-	0.08	0.28	0.80	1.04	1.72	1.84
PH2-0	(1. 39 mM)	16-Jul	0.01	0.11	0.07	0.48	1.29	0.66	1.82	0.51
PH2-3	(0. 23 mM)	5-Aug	0.01	0.02	0.04	0.15	0.41	0.08	0.59	0.18
PH2-7	(0. 26 mM)	5-Sep	0.02	0.15	0.02	0.04	0.11	0.02	0.21	0.15

*Ph2-7 represents the average concentration as measured during the seventh week of the second phase.

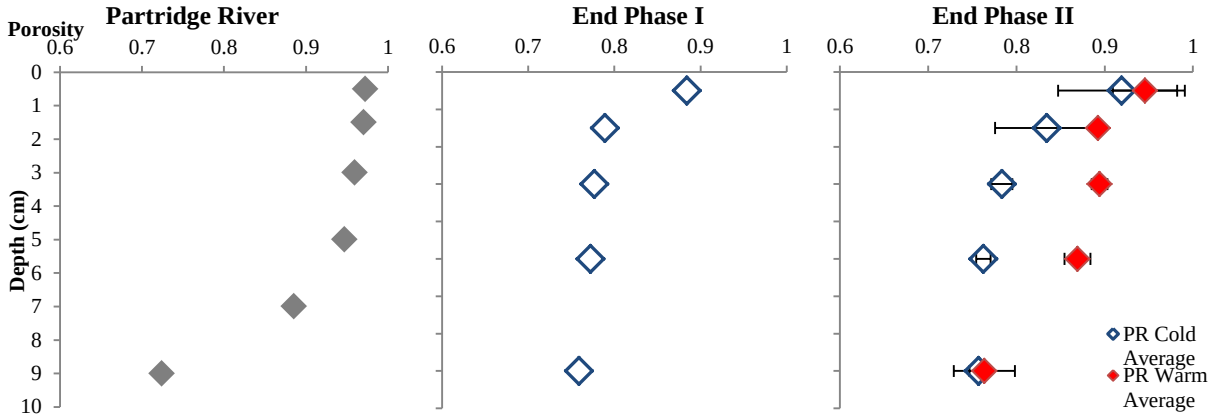

Figure 13 Partrige River Porosity measurements based on moisture content depth profile of (a) in- situ conditions, (b) mid-way through experiment, sacrificial microcosms, (c) porosity as measured in test microcosms at the end of the experiment.

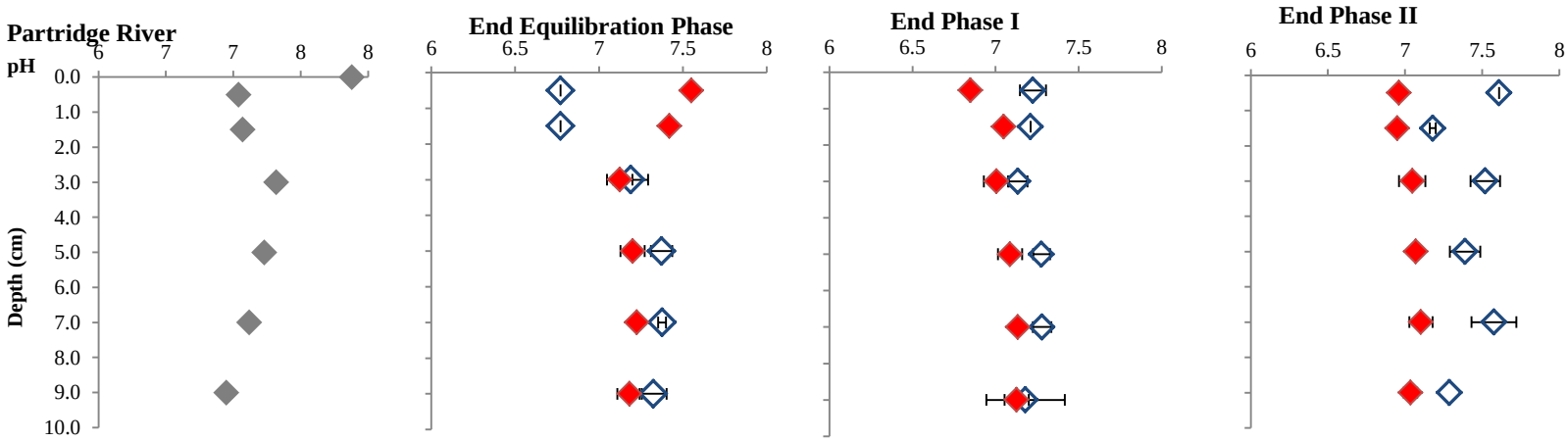

Figure 14 Partridge River porewater pH measurements taken at the end of each experimental Phase, (a) In situ conditions, (b) end of Phase I, (c) end of Phase I, (d) end of Phase II.

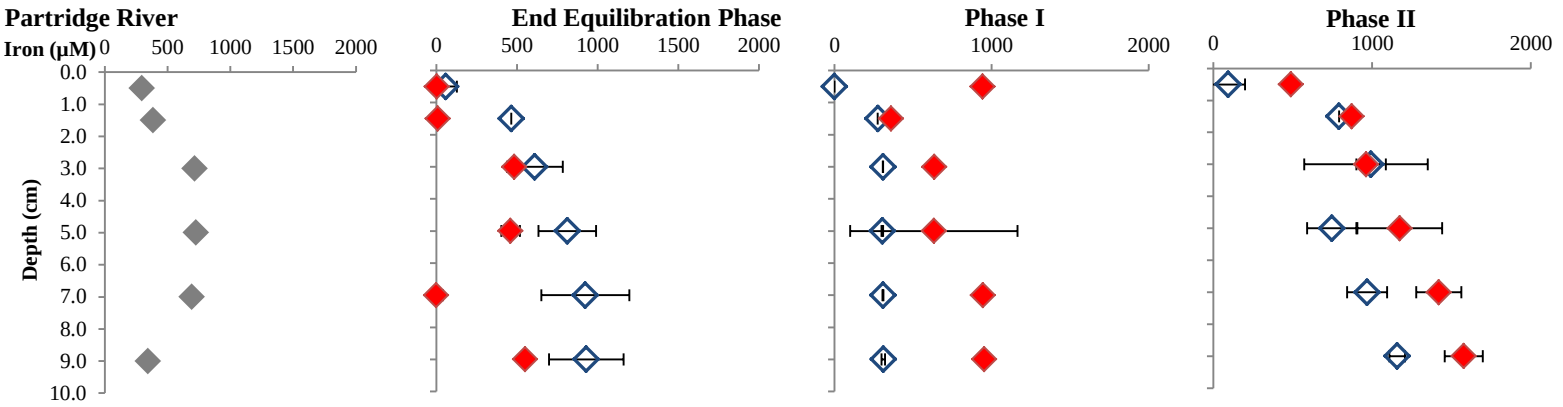

Figure 15 Partridge River porewater iron measurements, units are in micromole/L, (a) *In situ* conditions, (b) end of Phase I, (c) end of Phase I, (d) and end of Phase II.

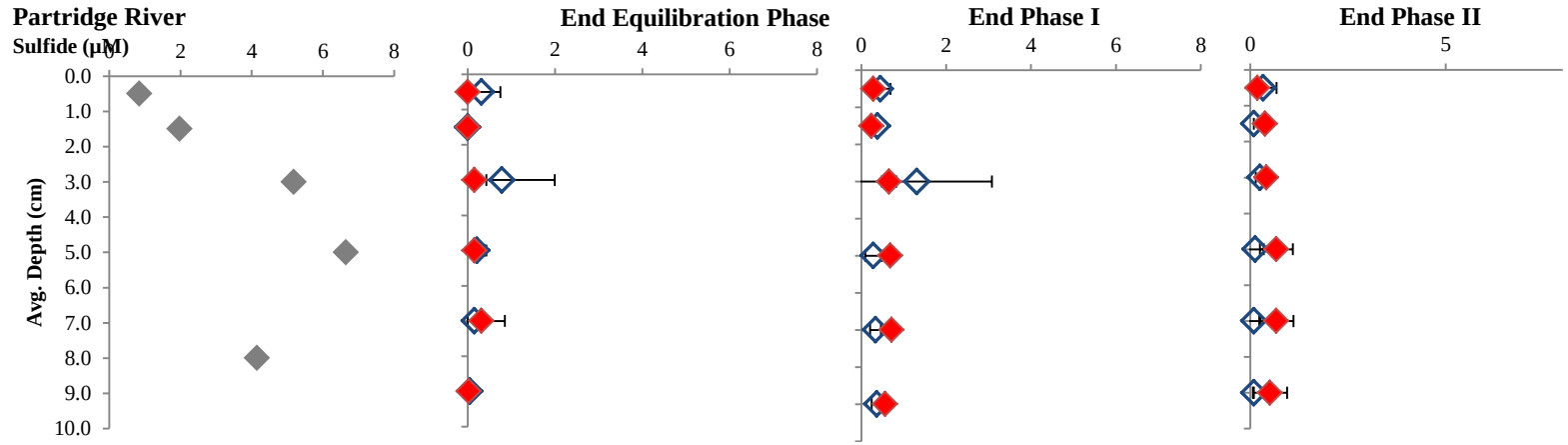

Figure 16 Partridge River porewater sulfide measurements, units are in micromole/L, (a) *In situ* conditions, (b) end of experimental Phase I, (c) end of Phase I, (d) endof experimetal Phase II.

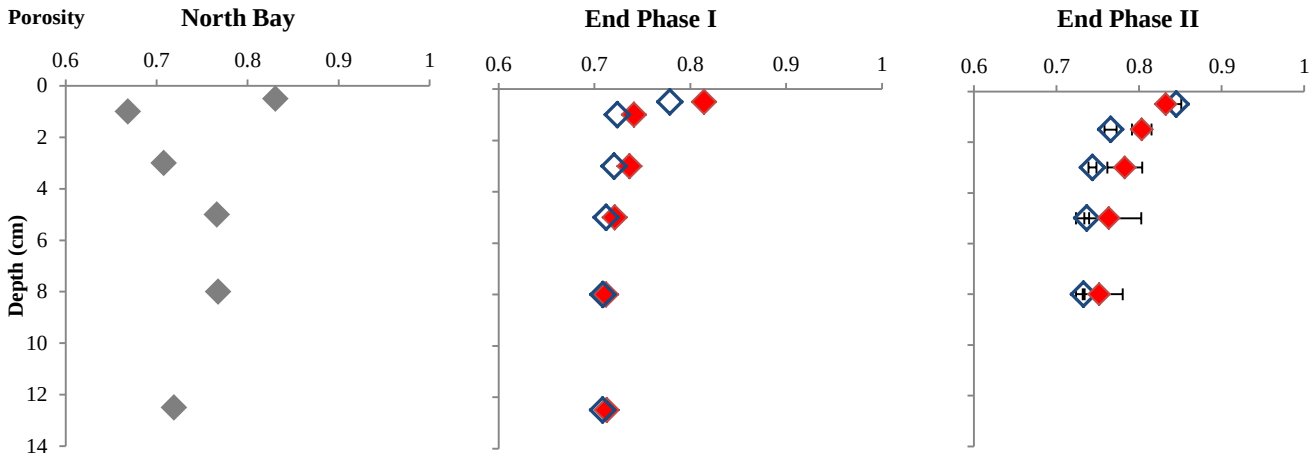

Figure 17 North Bay sediment porosity measurements based on moisture content depth profile of North Bay sediments, (a) in- situ conditions, (b) mid-way through experiment, sacrificial microcosms, (c) porosity as measured in test microcosms at the end of the experiment.

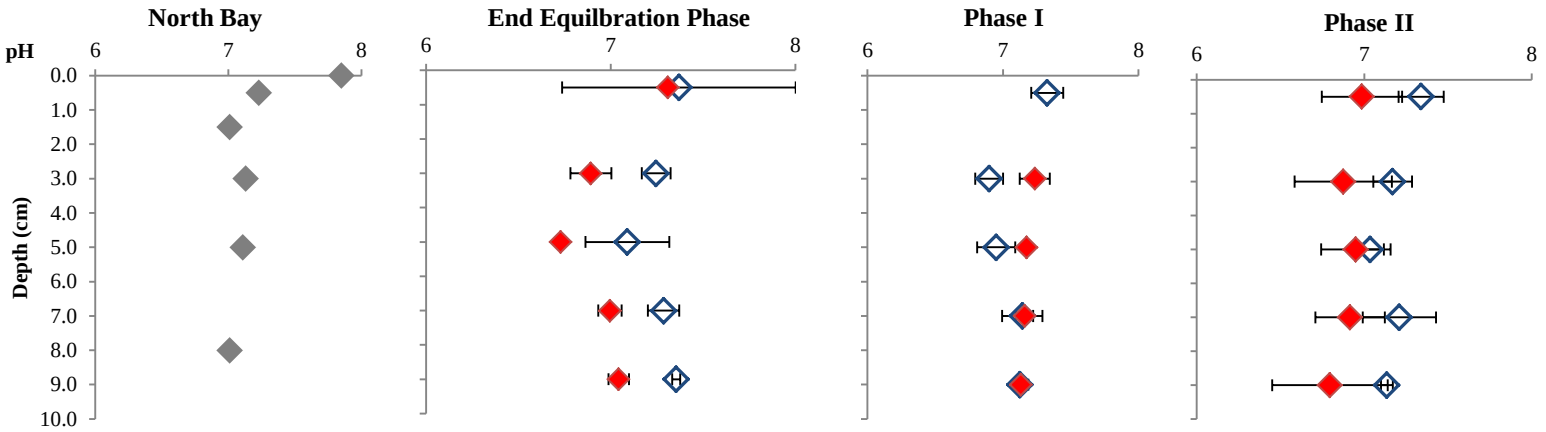

Figure 18 North Bay sediment pH measurements taken from North Bay porewater samples taken at the end of each experimental Phase, (a*)in situ* conditions ,(b) end of Phase I, (c) end of Phase I (d) end of Phase II.

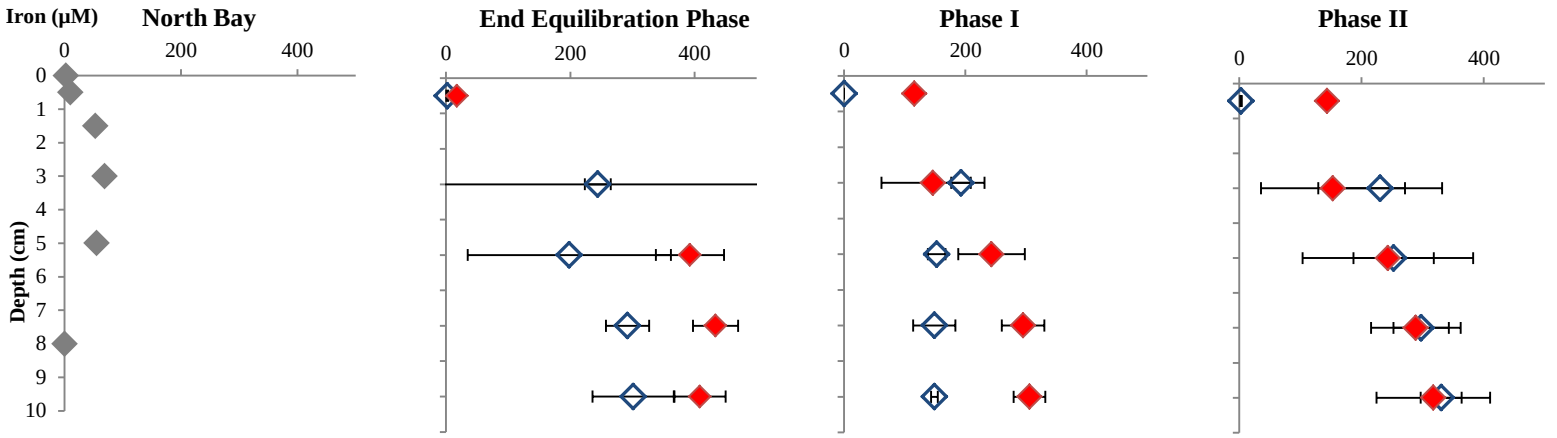

Figure 19 North Bay porewater iron measurements, units are in micromole/L, (a) *In situ* conditions, (b) end of Phase I, (c) end of Phase I, (d) and end of Phase II.

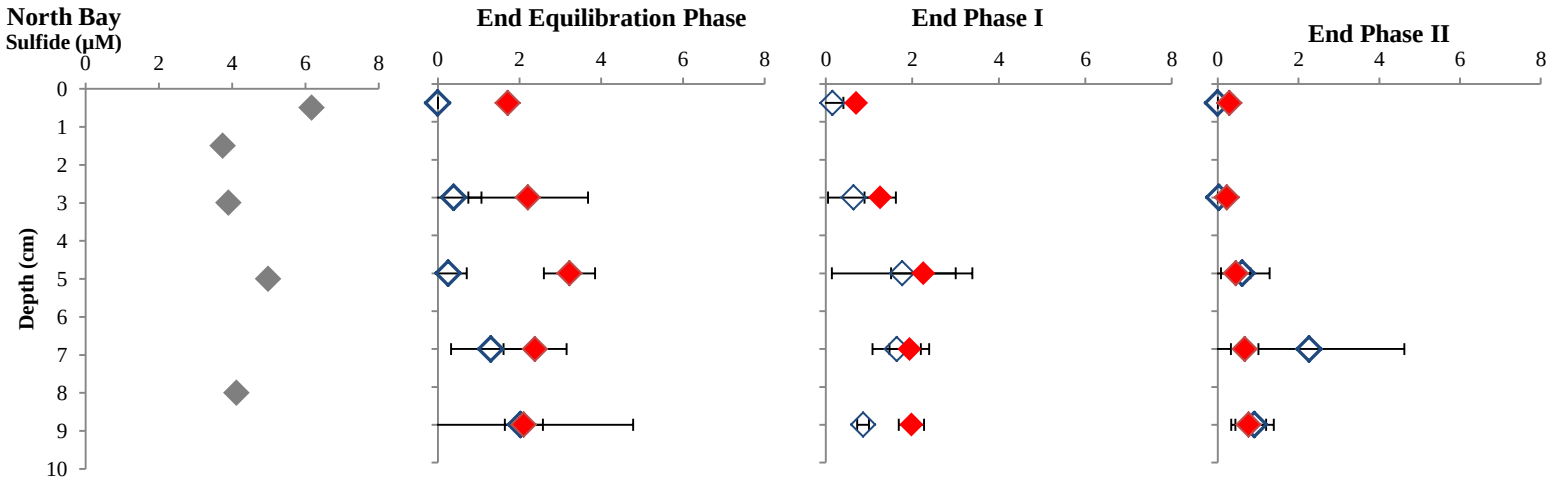

Figure 20 North Bay porewater sulfide measurements, units are in micromole/L, (a) *In situ* conditions, (b) end of Phase I, (c) end of Phase I, (d) end of Phase I.

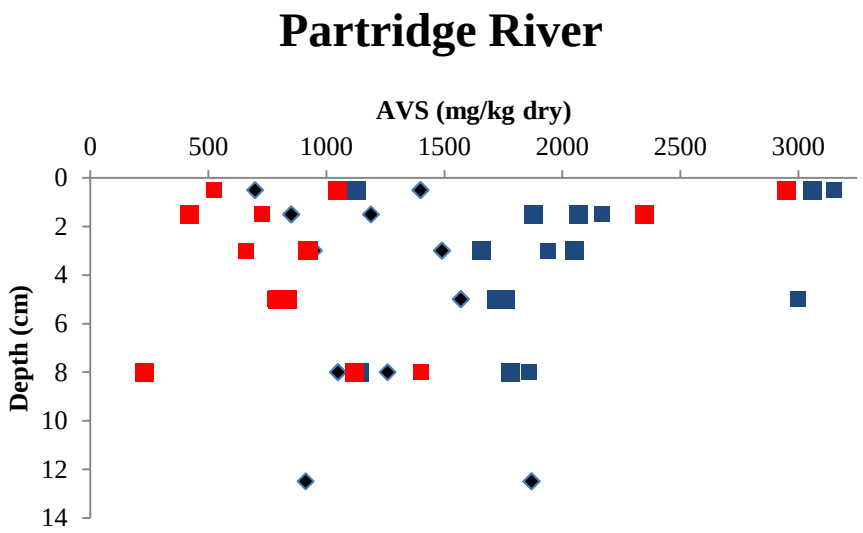

Figure 21 Partridge River AVS results for initial (black diamonds) final cold (blue square) and final warm (Red square)

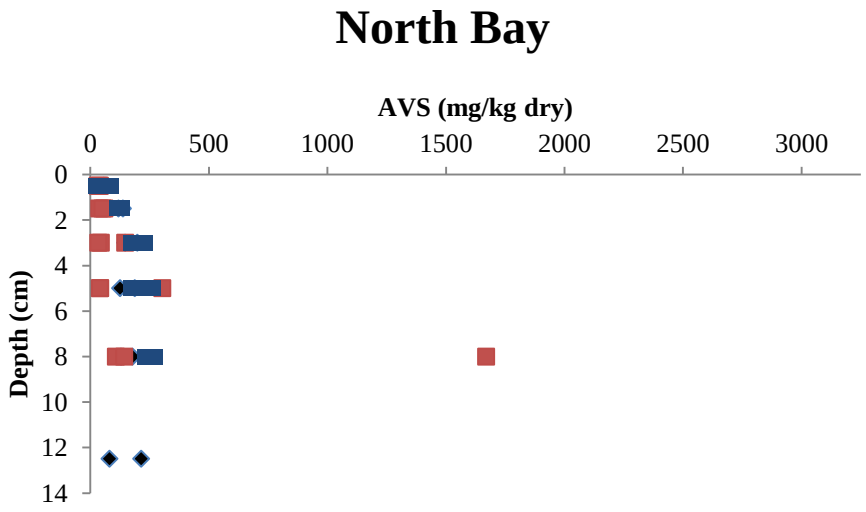

Figure 22 North Bay AVS results for initial (Black diamonds) Final cold (Blue Square) and Final warm (Red Square)

Appendix B

$$\boldsymbol{Porosity}^{*}(\boldsymbol{\varphi}) = \frac{\boldsymbol{W_w}}{\boldsymbol{\gamma_w}} / (\frac{\boldsymbol{W_s}}{\boldsymbol{\gamma_s}} + \frac{\boldsymbol{W_w}}{\boldsymbol{\gamma_w}})$$

γ_s=unit weight of soils (18kN/m^3 for North Bay sediment, 16kN/m^3 for Partridge River)
γ_w = the unit weight of water
W_s = the weight of solids in an individual sample
W_w = the weight of water
*porosity calculation assumes fully saturated conditions.

Appendix C.

$$\frac{R_{max} * C}{K_S + C} = Reaction\ rate \text{ (Monod, 1949)}$$

Table 15 Sulfate Reaction terms obtained from Pallude and Cappellen, 2005

Depth (cm)	$R_{max\_21°C}$ nmol cm^{-3} hr^{-1}	K_s mM
0-2	45. 5	0. 18
2-4	34. 0	0. 11
4-6	11. 2	0. 10
6-8	10. 7	0. 15